Biotransformation of 8:2 monosubstituted polyfluoroalkyl phosphate in rat & human liver, intestine, and fecal *in vitro* suspensions

By

Sampson Fok (Tsz Chun)

A thesis submitted to the Faculty of Graduate and Postdoctoral Affairs in partial fulfillment of the requirements for the degree of

Master of Science

in

Chemistry (Environmental and Chemical Toxicology)

Carleton University

Ottawa Ontario

Abstract

Polyfluoroalkyl phosphate esters (PAPs) have been used in many commercial and industrial applications due to their grease and water repellency, and surfactant properties. However, these compounds yield transformation products such as fluorotelomer alcohols (FTOHs) and perfluorinated carboxylic acids (PFCAs) that are environmentally persistent, bioaccumulative, and potentially toxic. Given that PAPs metabolize to bioactive products, it is important to understand the sites and kinetics of this metabolism. This research compares the biotransformation of a representative PAP, the 8:2 monosubstituted polyfluoroalkyl phosphate (8:2 monoPAP) in typical host biotransformation sites, the liver and intestine, to the mammalian microbiome. The 8:2 monoPAP was incubated in human and rat (male Sprague-Dawley) liver and intestine S9 fractions, and its immediate hydrolysis products, 8:2 fluorotelomer alcohol (8:2 FTOH) was monitored by GC-MS. Human and rat fecal samples were also collected, used as a surrogate for the gastrointestinal microbiome. Enzyme hydrolysis kinetics were measured and compared. Results show that the rat and human gut phosphatases have 2-fold and 1.3-fold more affinity for 8:2 monoPAP transformation, respectively ($K_{M\ (rat)} = (1.2 \pm 0.3) \times 10^3$ nM; $K_{M\ (human)} = (1.6 \pm 0.4) \times 10^3$ nM) compared to liver ($K_{M\ (rat)} = (4.0 \pm 1.5) \times 10^3$ nM; $K_{M\ (human)} = (4.9 \pm 3.3) \times 10^3$ nM). Results also show the microbiome contributes to 8:2 monoPAP hydrolysis. While the liver and intestine are the primary sites for metabolism, the microbiome plays a role and should not be overlooked. This may impact the relative risk of PAP exposure, given that levels of bioactive products, including PFCAs, may fluctuate depending on environmental and genetic factors leading to microbial diversity across individuals.

Acknowledgements

Firstly, I would like to express my sincere gratitude to my supervisor, Amy Rand, and research scientist, Todd Harris, for their guidance and mentorship throughout my MSc project. I remember starting off like a blank sheet of paper not knowing anything about research (didn't even know how to look up chemicals properly and took me weeks to find the product online), and progressed into confidently designing and troubleshooting experiments throughout the years. I would also like to thank Robert Letcher and Bill Willmore for taking the time to be in my MSc defense committee.

I would like to thank my parents for their continuous support, especially preparing me food care packages to bring back to Ottawa. There were many rough times during my MSc journey, and I wouldn't have made it through without their support. I also want to thank my brother, Freddy, for driving me back and forth between Ottawa and Markham during the COVID-19 period. You could have easily driven out from Montreal to Markham in 5 hours and made me take the train, but you took the time to detour into Ottawa to scoop me back to Markham. Really appreciate it!

To Jeff and Narr, thank you for being such supportive friends whenever I need advice and help. When I am back in Markham, we'll definitely go to Good Catch. To Priyank, we haven't seen each other ever since you moved to Ottawa for your undergrad. During my two years in Ottawa, you really took good care of me and I really appreciate you as a friend.

Lastly, I would like to thank my group members Dami, Colleen, and Keegan for their assistance and help throughout my research work. Especially Dami, you were my first buddy in the lab and without your presence, I would have struggled in many of my experiments. Again, thank you so much for your advice and help. To Morgan, I really thank you for your help with the fecal assays. I wouldn't have been able to prepare all those samples in one day if it weren't for you.

And to everyone else that supported me throughout this journey, I sincerely thank all of you!

Table of Contents

List of Tables

List of Figures

List of Supplementary Information Data

List of Abbreviations

Bicinchoninic acid	BCA
Bovine serum albumin	BSA
Disubstituted polyfluoro alkyl phosphate	diPAP
Fluorotelomer alcohol	FTOH
Fluorotelomer carboxylic acid	FTCA
Fluorotelomer unsaturated carboxylic acid	FTUCA
Gastrointestinal tract	GI tract
Half life	$T_{1/2}$
Intrinsic clearance level	CL_{int}
Monosubstituted polyfluoro alkyl phosphate	monoPAP
Mono[2-(perfluorooctyl)ethyl] phosphate	8:2 monoPAP
Per and polyfluoroalkyl substances	PFAS
Perfluorobutanoic acid	PFBA
Perfluorocarboxylate	PFCA
Perfluorodecanoic acid	PFDA
Perfluorohexanoic acid	PFHxA
Perfluorooctanoic acid	PFOA
Perfluorosulfonate	PFSA
Polyfluoroalkyl phosphates	PAPs
Trisubstituted polyfluoro alkyl phosphate	triPAP
Waste water treatment plant	WWTP
2-(Perfluoro-7-methyloctyl) ethanol	9ME 8:2 FTOH

1.0 Overview

Per- and polyfluoroalkyl substances (PFAS) are chemicals used in many industrial applications and household products, including fire extinguisher foams, textiles, household cleaning agents, non-stick cookware, and food packaging materials [1,2]. Their manufacturing and use has also led to their detection in drinking water [3], wastewater sludge [4], household dust [5], and human blood serum [6]. A total of 4730 different types of PFAS compounds are currently identified in manufacturing and environment occurrences [7]. PFAS are environmental and health concerns given that some classes are persistent, bioaccumulative, and resistant to environmental and biological transformation [8–10]. For example, perfluorosulfonates (PFSAs) compounds have been shown to be more bioaccumulative than perfluorocarboxylates (PFCAs) [11]. Although there is no explanation as to why PFSAs are more bioaccumulative than PFCAs, it has been shown that longer bioaccumulation potential and persistency is correlated with increased chain length [11]. PFAS are aliphatic compounds that contain a hydrophobic fluorinated tail and a hydrophilic head [1]. PFAS can be categorized into perfluoroalkyl substances and polyfluoroalkyl substances [1]. The hydrophobic tail of perfluoroalkyl substances have fluorine atoms attached to all of the carbon atoms, while the hydrophobic fluorinated tail of polyfluoroalkyl substances have at least one carbon attached to hydrogen atoms [1], illustrated in Figure 1.1. The goal of this thesis was to examine the transformation of a commercial fluorinated surfactant commonly found in human blood. Specifically, the contribution of hepatic and non-hepatic biotransformation (e.g. intestine, microbiome) are examined to characterize the relative kinetics involved in forming bioactive and persistent per- and polyfluorinated metabolites. Table 1.1 lists the names, structures, and abbreviation of various PFAS that are of interest to this work.

Perfluoroalkyl substances	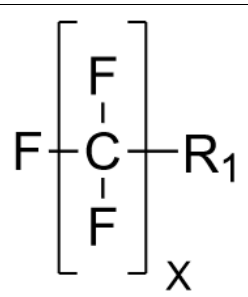
Polyfluoroalkyl substances	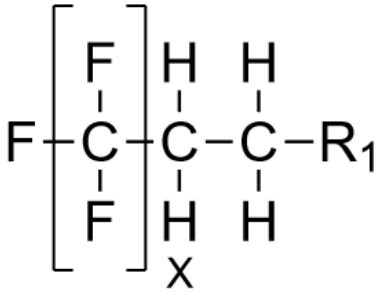

Figure 1.1: General structure of per- and polyfluoroalkyl substances. Where R_1 can be several polar functional groups, including -OH, -PO_4, -COOH, -SO_3.

Name	Acronym	Structure
Monosubstituted polyfluoroalkyl phosphates	X:2 monoPAPs	$CF_3(CF_2)_{x-1}CH_2CH_2O\text{-}P(O)(OH)_2$, x = 8
Fluorotelomer alcohol	X:2 FTOH	$CF_3(CF_2)_{x-1}CH_2CH_2OH$, x = 8
Fluorotelomer secondary alcohol	X:2 sFTOH	$CF_3(CF_2)_{x-1}CH(OH)CH_3$, x = 7
Fluorotelomer aldehydes	X:2 FTAL	$CF_3(CF_2)_{x-1}CH_2C(O)H$, x = 8
	7:3 β-keto Aldehyde	$CF_3(CF_2)_6C(O)CH_2C(O)H$
Fluorotelomer unsaturated aldehydes	X:2 FTUAL	$CF_3(CF_2)_{x-2}CF = CHC(O)H$, x = 8
Fluorotelomer ketone	X:2 Ketone	$CF_3(CF_2)_{x-1}C(O)CH_3$, x = 7
Fluorotelomer carboxylic acid	X:2 FTCA	$CF_3(CF_2)_{x-1}CH_2COO^-$, x = 8
	X:3 FTCA	$CF_3(CF_2)_{x-1}CH_2CH_2COO^-$, x = 7
Fluorotelomer unsaturated carboxylic acid	X:2 FTUCA	$CF_3(CF_2)_{x-2}CF = CHCOO^-$, x = 8
	X:3 FTUCA	$CF_3(CF_2)_{x-1}CH = CHCOO^-$, x =7
Perfluoroalkyl carboxylic acid	PFCA	$CF_3(CF_2)_{x-1}COO^-$, x = 7,8,9
Perfluorononanoic acid	PFNA	$CF_3(CF_2)_7COO^-$
Perfluoroheptanoic acid	PFHpA	$CF_3(CF_2)_5COO^-$

Table 1.1: Names, structures, and abbreviation of various PFAS of interest to this work. Name, acronym and structural formula were obtained from Butt *et al.* [12].

1.1 Polyfluoroalkyl phosphate esters (PAPs)

One class of PFAS are the polyfluoroalkyl phosphate esters (PAPs), which are applied to food packaging materials to impart grease-resistance [13,14]. PAPs have been found in popcorn bags [13,15], fries and burger boxes [13], baking papers [13], and pizza grease proof papers [13]. The PAPs can be further divided into subclasses based on the number of ester functionalities and length of their fluorinated chain, as shown in Figure 1.2. PAPs have a chain length nomenclature of X:2, where X indicates the number of fluorinated carbons and 2 indicates the hydrogenated carbon atoms [1]. These PAPs are commonly found in the 4:2−12:2 form [16,17]. Furthermore, PAPs can have mono-, di-, or tri-substituted polyfluorinated chains (monoPAP, diPAP, and triPAP, respectively) [1,15–17].

While PAPs have been detected as monoPAP, diPAP, and triPAP in consumer products [15], the 6:2 and 8:2 diPAP are congeners found at highest levels in both food packaging materials [13] and human serum [18]. For example, the 6:2 and 8:2 diPAP have been found at 0.67 ng and 0.32 ng in popcorn bags [13]. Levels of 6:2 and 8:2 diPAP ranged from < 0.018 − 0.14 ng/mL and < 0.009 − 0.11 ng/mL in a study looking at 61 human serum samples collected in the Norway [18]. These food packaging materials may be sources of dietary PAP exposure given their propensity to migrate into consumer's foods [19].

Name	Structure
monoPAP	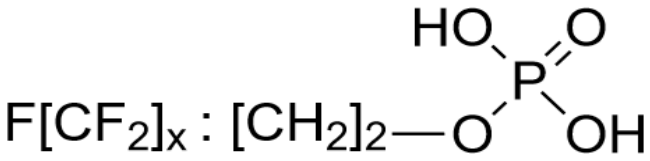
diPAP	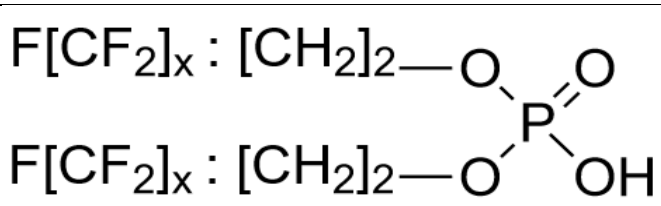
triPAP	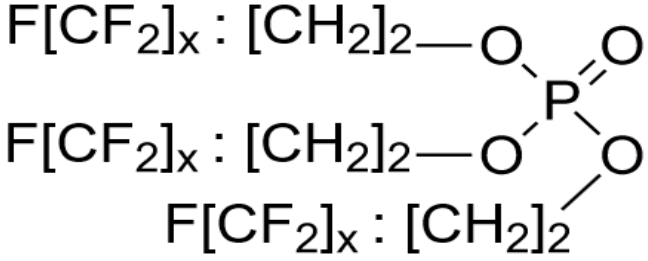

Figure 1.2: Structures of X:2 mono-, di-, or tri-substituted polyfluoroalkyl phosphates (PAPs), where X represents the number of fluorinated carbons, commonly ranging from 4-12.

1.1.1 The chemical stability of PFAS

The hydrophobic tail and hydrophilic head of PFAS make these compounds favourable for commercial and industrial applications [1,2]. Specifically, the unique thermal stability of PFAS is due to the fluorine element [2]. The high electronegativity and low polarizability of fluorine allows it to form a strong covalent bond with carbon [2]. In fact, the carbon-fluorine bond (116 kcal/mol) is one of the strongest covalent bonds compared to the carbon-hydrogen bond (99.5 kcal/mol) [2,20]. Another factor contributing to the stability of PFAS are the many fluorine atoms within the hydrophobic tail [2]. Because of the valence electrons surrounding the fluorine atom, this makes the hydrophobic tail very bulky and sterically hindered, which is unfavourable for nucleophilic attacks to the carbon [2,21], as illustrated in Figure 1.3.

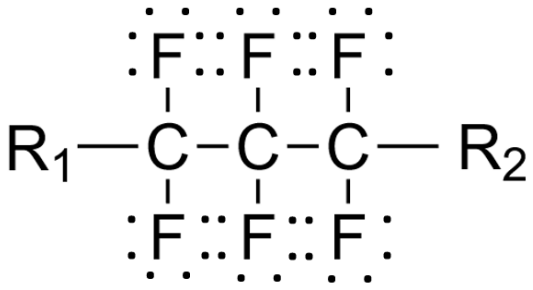

Figure 1.3: Steric hinderance around the fluorine atom.

Although PFCAs and PFSAs are the most stable surfactants, not all PFAS are thermally stable [2]. Even with the grease-resistant properties of PAPs [13,14], they have been shown to have reduced stability and can undergo abiotic and biological transformations due to the electrophilic nature of their polar head group, making them susceptible to phosphate ester hydrolysis.[1,16,17,22].

Biotransformation pathway of 8:2 monoPAPs

The biotransformation pathway of PAPs has been well established (Figure 1.4). The PAPs undergo transformation first through hydrolysis of the phosphate ester to form a fluorotelomer alcohol (FTOH), then intermediate metabolites fluorotelomer carboxylic acid (FTCA) and fluorotelomer unsaturated carboxylic acid (FTUCA), followed by α- and β-like oxidation mechanisms to form PFCAs [16,22,23]. Lee et al. explored the biodegradation of 8:2 monoPAP in a simulated waste water treatment plant (WWTP) environment and observed primarily 8:2 FTOH in the headspace of the bottle while the aqueous phase consisted of 8:2 FTCA followed by 8:2 FTUCA and perfluorooctanoic acid (PFOA) [22]. The degradation of 4:2, 6:2, and 10:2 monoPAP in WWTP sludge yielded analogous products corresponding to their respective chain lengths. [22]. Biotransformation of 4:2−10:2 mono and diPAPs, was also investigated in rats, where their respective FTOH, FTCA, FTUCA, and PFCA metabolites were observed in the blood [16,17]. In addition, the 6:2−10:2 mono- and diPAPs were observed in feces after oral gavage, suggesting that a fraction of these compounds do not undergo transformation and are eliminated [17]. A follow up study by Jackson and Mabury demonstrated that monoPAPs can undergo extrahepatic transformation, by hydrolyzing to FTOHs in the presence of gut phosphatase enzymes in approximately 1.5 minutes [24].

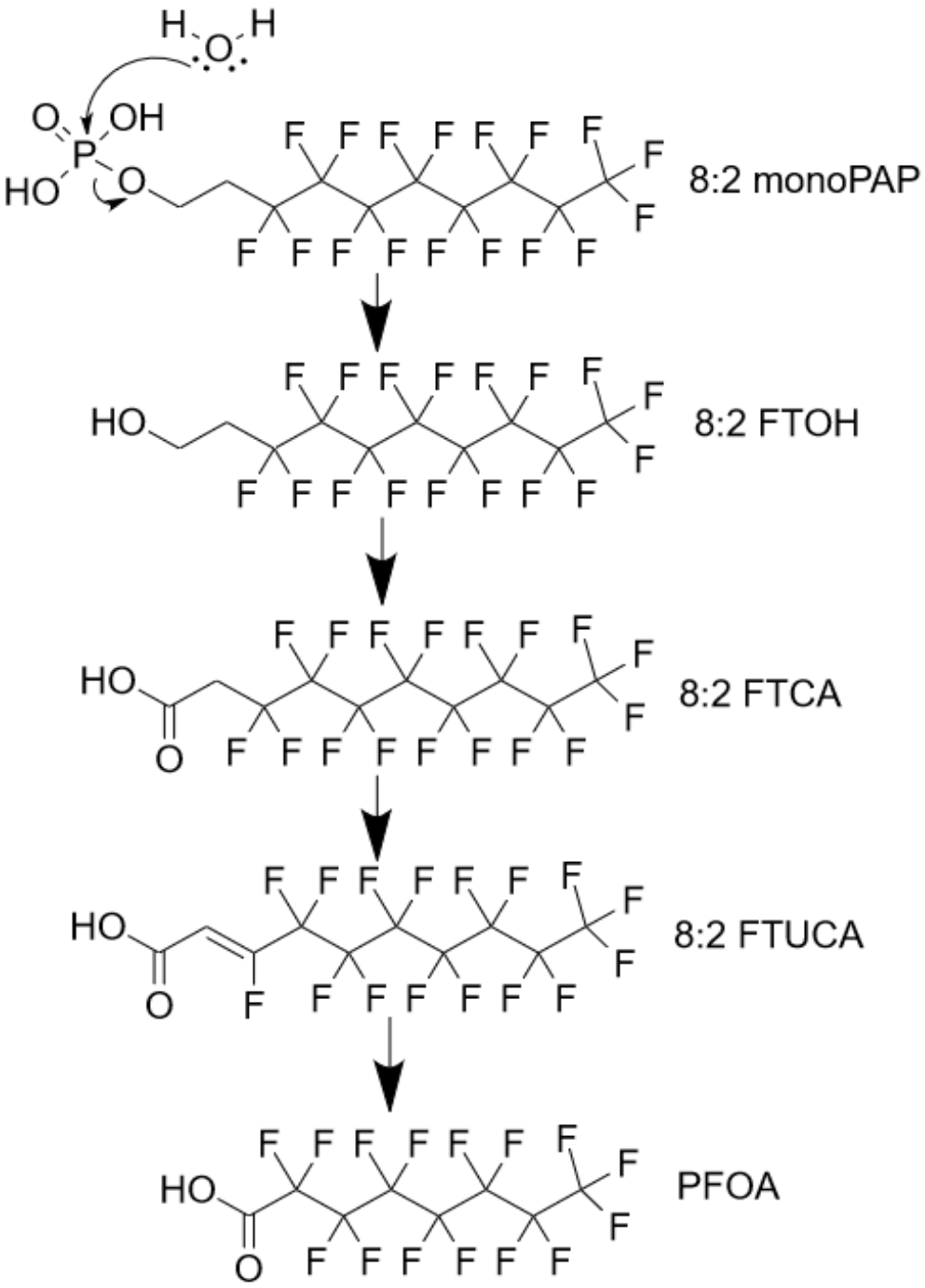

Figure 1.4: General biotransformation pathway of 8:2 monoPAP.

Elimination and half life of PAPs

In recent years, industries have phased out longer chain PFAS (≥ 8 carbons) to shorter chain PFAS (≤ 6 carbons) due to reduced bioaccumulation [25,26] and toxicity [4,27]. While their mechanism of toxicity is similar to longer chain PFAS [28], short chain PFAS are considered less toxic due to the shorter *in vivo* half lives [29] and increased clearance rates [30]. In WWTP microbial environment, the rate of FTOH production decreased as the length of monoPAP chain increased;the number of days for monoPAP to be fully transformed to FTOH was lower for short chained monoPAP than long chained monoPAP, illustrated in (Table 1.2) [22].

Table 1.2: Number of days required for the various chain length monoPAPs to fully transform into FTOH in a WWTP microbial environment [22].

Substrate (X:2 monoPAP)	Transformation product (X:2 FTOH)	Number of days required for full transformation of substrate to product
4:2 monoPAP	4:2 FTOH	1 day
6:2 monoPAP	6:2 FTOH	40 days
8:2 monoPAP	8:2 FTOH	50 days

While transformation was reported in WWTP microbial environment [22], high concentrations of diPAP are found in the blood serum and a similar trend can be seen in a rat model examining PAPs chain length and half life [16,17]. Nonetheless, both monoPAP and diPAP are transformed into PFCAs which is concerning because PFCAs tend to have a longer half life compared to their parent compounds, illustrated in Table 1.3 [17]. For example, in rats the 8:2 diPAP half life is about 5-times less than the major PFCA metabolite, PFOA [17]. In human, PFOA has a half life of about 3.8 years [31]. Although there

346 is no available data regarding the half life of diPAP in humans, we can predict with similar trends that

347 PFCAs will have longer half-lives than diPAPs.

348

PAPs precursor	Rats ($T_{1/2}$)	Hydrolysis product	Rats ($T_{1/2}$)	Major PFCA product	Rats ($T_{1/2}$)	Humans ($T_{1/2}$)
4:2 diPAP	1.6 days [17]	**4:2 FTOH**	1.1 - 1.7 hours [32]	**PFBA[a]**	3.3 days [17]	74 hours [33]
6:2 diPAP	2.1 days [17]	6:2 FTOH	Undetermined	**PFHxA[a]**	1.8 days [17]	32 days [34]
8:2 diPAP	4.8 days [17]	8:2 FTOH	Undetermined	**PFOA[a]**	23 days [17]	3.8 years [31]
10:2 diPAP	3.3 days [17]	10:2 FTOH	Undetermined	**PFDA[a]**	10 days [17]	n/a

349 **Table 1.3:** Half-lives of various PAPs and their oxidation products in rat and human [15,29,30,31,32].

350 Note: [a]Perfluorobutanoic acid (PFBA), Perfluorohexanoic acid (PFHxA), Perfluorooctanoic acid

351 (PFOA), Perfluorodecanoic acid (PFDA).

352

1.1.2 Metabolism in the S9 fraction

The S9 cellular fraction is often used to model the biotransformation of xenobiotics as it contains many of the phase I and phase II enzymes responsible for metabolism [35]. The hepatic S9 fraction can be obtained by low speed centrifugation (at 9000 x *g*) from liver homogenate to separate the mitochondria and the lyposomes [35,38]. Further high speed centrifugation (e.g. 100 000 x *g*) of the S9 fraction can yield the cytosol (containing soluble enzymes) and microsomes (containing membrane bound enzymes) [35,38] (Figure 1.5). The microsome fraction contains CYP450 enzymes that are responsible for phase I metabolism, while the cytosol fraction consists of enzymes responsible for phase II metabolism [35]. Because the S9 fraction is comprised of microsome and cytosol, it can provide a comprehensive environment to monitor both phase I and II metabolism [36].

Aside from the liver, S9 fractions can also be obtained from the intestine [37]. Because first pass metabolism in the intestinal wall can affect the bioavailability of drugs entering the liver, the possibility of intestinal metabolism cannot be excluded [38]. Literature has reported that the intestine contains phase I and II enzymes that also contribute to metabolism and transport [39].

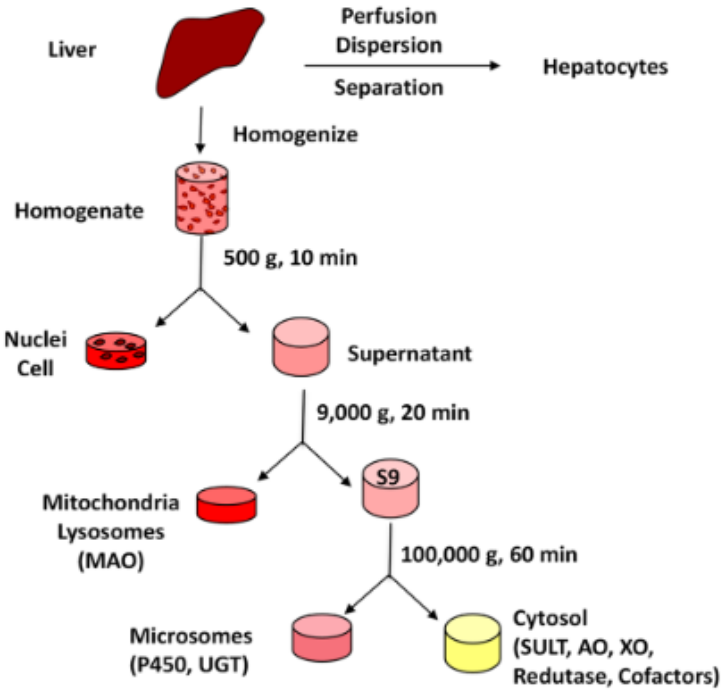

Figure 1.5: Separation of S9, microsome, and cytosol fractions from liver homogenate. Figure obtained from Dennis *et al.* [40]

Following absorption, the drug or toxicant is transported to the liver for detoxification [41]. The purpose of phase I metabolism is to transform the drug or toxicant into a chemically reactive intermediate more susceptible towards phase II metabolism, and/or more polar and readily excretable[41]. The biotransformation reactions that occur in phase I metabolism include oxidation (hydroxylation, deamination, dealkylation, and dehydrogenation), reduction, and hydrolysis [41]. In phase II metabolism, the goal is to make the reactive intermediate in phase I more polar and water soluble for excretion through conjugation [41]. Common conjugation reactions include glucuronidation, sulphation, acetylation, and glutathione addition [41]. Following phase II metabolism, hydrophilic conjugated products can be excreted through the kidney into urine [41]. Lipophilic conjugated products can be excreted into the bile, where they can be reabsorbed by the intestine for further metabolism, or directly excreted into the feces [41] (Figure 1.6).

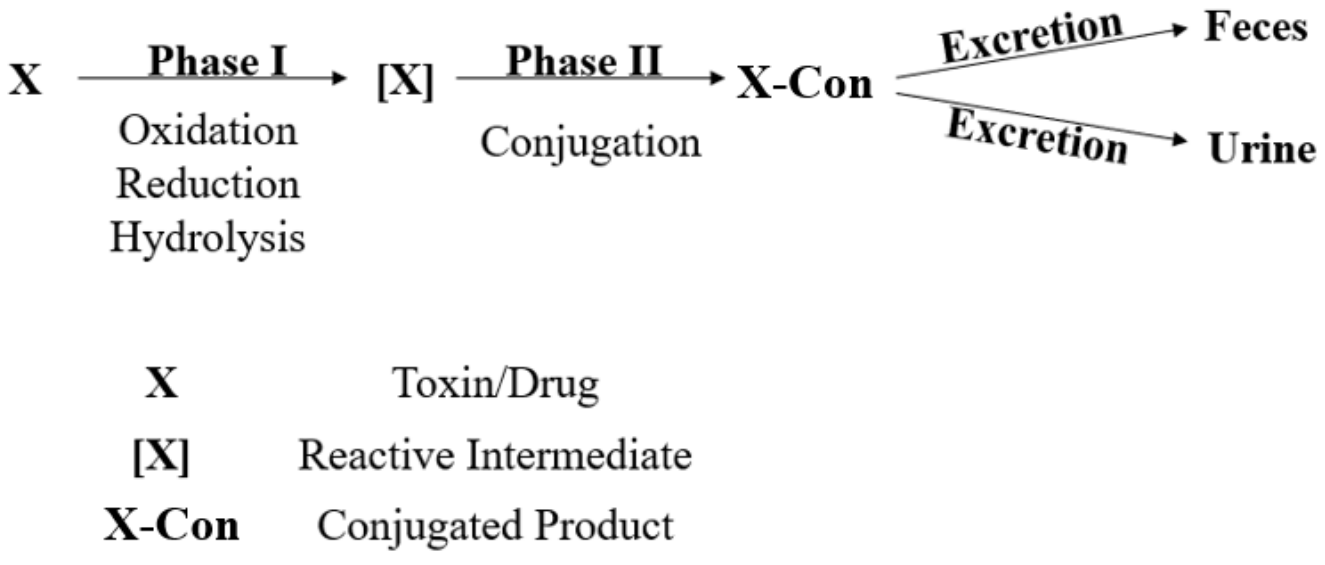

Figure 1.6: Phase I and II metabolism pathways

1.2.3 Fecal microbiome biotransformation

As described above in section 1.2, PAPs undergo microbial and mammalian (gut and liver) biotransformation. They also do not fully transform and have been found in their unchanged form in feces [17]. Given the presence of PAPs in rat feces, a proxy for their presence in the large intestine, it is a reasonable hypothesis that PAPs may also be substrates for microbiota within the gastrointestinal (GI) tract. The human gastrointestinal tract is a complex system estimated to contain over 1000 types of microbial species [42]. Due to this diversity, several studies have examined the contribution of the human microbiome to xenobiotic metabolism, where mechanisms include hydrolysis [43–45], nitro-reduction [45,46], hydroxylation [45,47], and methylation [45,48]. Furthermore, gut microbiome based therapeutics have been of particular interest in drug industries [49] as the gut microbiome can activate and deactivate drugs, and generate reactive intermediate drug metabolites [50]. For example, Famciclovir, Roxatidine acetate, and Vilazodone are activated upon hydrolysis of their ester or amide group by Bacteroidetes in the human

microbiome [51]. Given that microbes present in our gastrointestinal tract can hydrolyze drugs, we hypothesize that the microbiome plays an important role in the transformation of PAPs.

1.2 Biochemistry

The biochemistry of enzyme kinetics allows us to determine the rates at which 8:2 monoPAP is biotransformed into 8:2 FTOH, and compare the rates between liver, intestine, and fecal microbes in both the rat and human.

1.2.1 Enzymatic reactions

An enzyme is a catalytic protein that contains an active site, allowing a substrate to bind and transform into a product, sometimes aided by a co-factor [52], as illustrated in Figure 1.7. Initially, the enzyme will contain an open active site which allows a substrate of interest to bind to the catalytic site, forming an enzyme-substrate complex [52]. This enzyme-substrate complex will undergo a reaction to form a enzyme-product complex [52]. Lastly, the product is released from the enzyme active site [52].

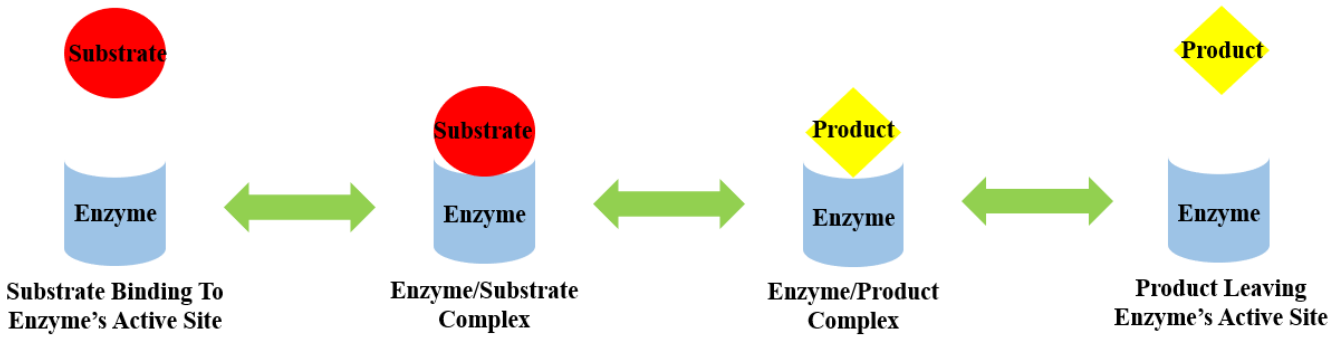

Figure 1.7: Enzyme catalyzed reaction of substrate to product. Adapted from Liu 2012 [52].

1.2.2 Michaelis Menten Kinetics

The enzymatic reaction diagram above can be expressed in the following reaction equation scheme below, where E, S, ES, and P are enzyme, substrate, enzyme-substrate, and product, respectively [52]. K_1, K_{-1}, and K_2 are the rate constants for the enzymatic reaction [52].

$$E + S \underset{K_{-1}}{\overset{K_1}{\rightleftharpoons}} ES \xrightarrow{K_2} E + P$$

The rate of product formation can be expressed in the following term [52].

$$V_o = K_2[ES]$$

With the steady state approximation, we can assume that the rate of enzyme-substrate formation is in equilibrium with the rate of enzyme substrate dissociation [52].

$$K_1[E][S] = (K_{-1} + K_2)[ES]$$

Following further complex mathematical derivatization from the enzymatic reaction equation, we generate the Michaelis-Menten equation below, where V_o, V_{max}, K_M, and [S] are the velocity (or rate), maximum velocity achieved by the system, Michaelis-Menten constant, and substrate concentration, respectively [52].

$$V_o = \frac{V_{max}\,[S]}{[S] + K_M}$$

We can express the Michaelis-Menten equation using a Michaelis-Menten kinetic plot (Figure 1.8).

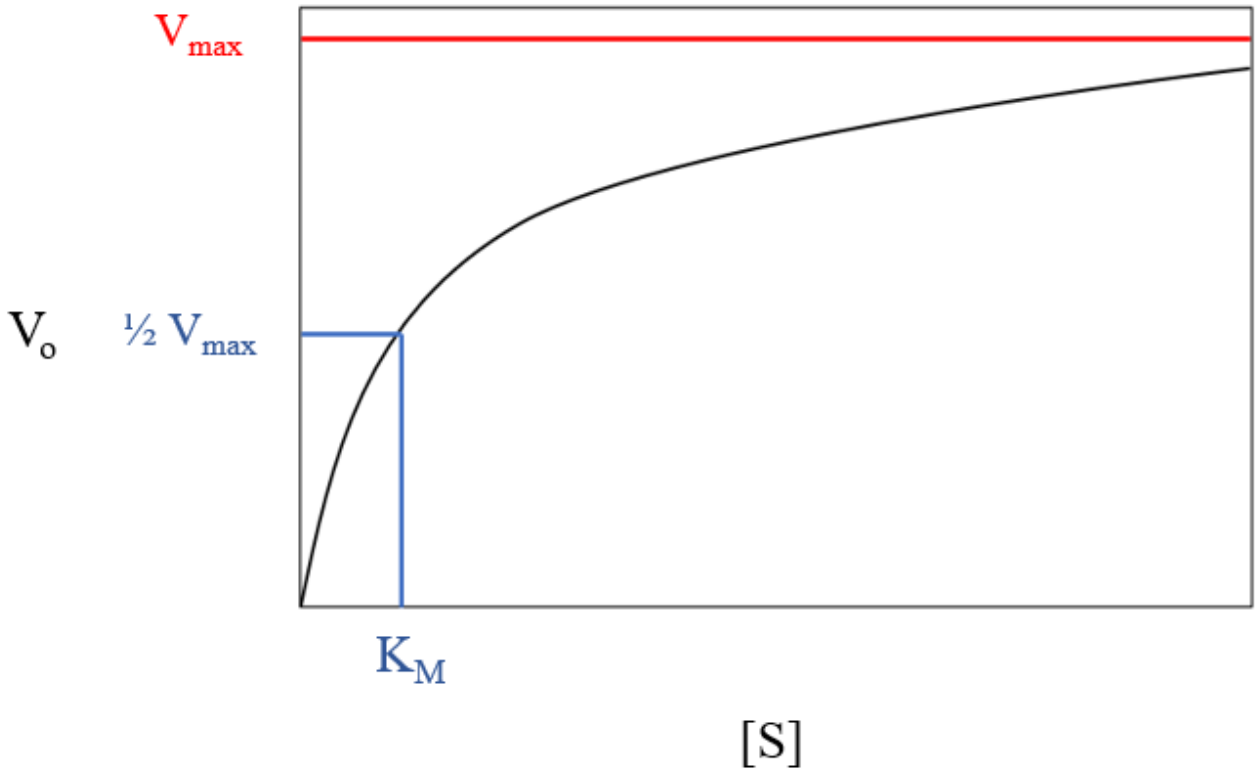

Figure 1.8: Michaelis-Menten kinetic plot.

V_{max} is the maximum velocity in which the enzyme catalytic site is occupied with the maximum number of substrate molecules and K_M is the substrate concentration which is required to reach half V_{max}. A low K_M indicates that a small substrate concentration is required to reach half V_{max} as there is a high binding affinity between the enzyme and substrate to form the enzyme-substrate complex [53]. Conversely, a large K_M indicates that a large substrate concentration is required to reach half V_{max} as there is a low binding affinity between the enzyme and substrate to form the enzyme-substrate complex [53].

1.2.3 K_{cat}/K_M and V_{max}/K_M

The V_{max} is also used to determine the K_{cat} value, which is the turnover number of an enzyme [53]. The turnover number is defined as the maximum number of substrates that one enzyme is capable of

440 catalyzing into products per unit time [53]. Under the assumption of when the substrate concentration is
441 below the K_M value, the K_{cat}/K_M value describes how efficient the enzyme is capable of catalyzing the
442 substrate, which can be described in the following equation below [53].

443 $$V_o = \frac{K_{cat}}{K_M}[S][E]_{Total}$$

444 Because the substrate concentration is very low and the number of unoccupied enzymes approximate the
445 total enzyme in the system, $[E]_{Total}$, the K_{cat}/K_M ratio is the rate constant that can be used to describe the
446 enzyme efficiency [53]. This K_{cat}/K_M value is also defined as the catalytic efficiency [53]. The K_{cat}/K_M value
447 is particularly important when comparing the kinetics of different substrates metabolized by the same
448 enzyme.

449 In an *in vitro* kinetic model, enzyme efficiency can be described in the intrinsic clearance of a
450 drug (CL_{int}), which is a ratio between V_{max}/ K_M [54]. This ratio provides a better prediction of enzyme
451 metabolism for the total organ such as the liver [54]. The CL_{int} is particularly important when comparing
452 the kinetics of a single substrate metabolized by different enzymes.

453 **1.4 Study objective**

454 The objective of this study was to determine whether 8:2 monoPAP biotransforms to 8:2 FTOH
455 within the rat and human microbiome. Using 8:2 monoPAP as a probe substance, we examine the
456 relative contribution that fecal microorganisms play in PFAS metabolism, comparing the metabolic rates
457 to enzyme catalysis from liver and intestine.

458

459

2.0 Materials and Methods

2.1 Ethics

The human ethics application was approved by the Carleton University Research Ethics Board-B (Clearance #112094). Participants were aged 18 years or over, without history of gastrointestinal disorders, and were free from antibiotics within the past three months from collection point.

2.2 Chemicals

Mono[2-(perfluorooctyl)ethyl] phosphate (8:2 monoPAP) and the 2-(Perfluoro-7-methyloctyl)ethanol (9ME 8:2 FTOH) internal standard were obtained from Toronto Research Chemicals (97% pure; CAS# M566820) and Oakwood Products Inc (98.9% pure, CAS# 31200-98-3) respectively. Methanol (≥ 99.8% pure; HiPerSolv Chromanorm), and ethyl acetate (≥ 99.8% pure; ACS) were purchased from VWR. Sodium dihydrogen phosphate monohydrate (99% pure; biotechnology grade) and sodium phosphate dibasic anhydrous (99.5% pure; biotechnology grade) were purchased from Bioshop Canada Inc. Pooled male Sprague-Dawley rat liver S9 fractions were purchased from Sigma-Aldrich. PMSF-free pooled male Sprague-Dawley rat and mixed gender human S9 intestine fractions, and pooled mixed gender human liver S9 fractions were obtained from Sekisui XenoTech. The bicinchoninic acid assay kit for protein quantification was obtained from Thermo Fisher Scientific.

2.3 Incubation of 8:2 monoPAP in rat and human liver and intestine S9 fractions

The S9 incubation method was obtained from Butt et al. with minor modifications [55]. The 8:2 monoPAP stock solution was prepared in methanol (5 mg/mL) and diluted in water such that the final concentration of methanol was ≤0.1% of the total incubation volume. Phosphate buffer (0.1 M, pH 7.4) was added to 1.5 mL microcentrifuge tubes in a water bath at 37 °C and preheated for 5 minutes. An aliquot of S9 (0.5 mg/mL) was then added to each microcentrifuge tube, incubating for 1 minute.

Reactions were initiated with 8:2 monoPAP (concentrations ranging between 400 – 7000 nM) and incubated up to 2.5 mins (time points were taken 0, 0.5, 1, 1.5, 2, and 2.5 mins). The final reaction volume containing buffer, S9, and 8:2 monoPAP was 500 µL. The reactions were terminated at each time point with ethyl acetate (500 µL) containing 1 µM of the 9ME 8:2 FTOH internal standard, vortexed for 2 minutes, and centrifuged at 5000 rpm for 5 minutes at room temperature. The ethyl acetate layer was removed from the aqueous layer, transferred to GC-MS amber glass vials, sealed and stored at -20 °C until GC-MS analysis.

2.4 Incubation of 8:2 monoPAP in rat and human feces

Rat and human feces were used to investigate the microbiome contribution to PAPs metabolism as the majority of the bacteria are situated in the large intestine [56]. Examining metabolism within feces was a proxy for the endogenous metabolism that occurs in the large intestine [57], as it contains the same microflora that are present in the large intestine [56,57]. The collection and incubation procedures were obtained from McCabe et al. with minor modifications [57]. Male rat fecal samples were donated by the University of Ottawa Animal Care and Veterinary Service and stored at -80 °C until use. Human fecal samples were collected from 1 male and 1 female participants, pooled, and brought to anaerobic conditions within 2 hours after collection to prolong bacterial lifetime [58]. Samples were added to phosphate buffer (0.1 M, pH 7.4) to a final concentration of 0.1 g wet weight/mL. This mixture was homogenized, then centrifuged at 500 rpm for 5 minutes to remove particulates. The supernatant was transferred to a new 50 mL falcon tube.

The rat fecal experiment was performed aerobically to demonstrate a proof of concept that fecal microbes can metabolize 8:2 monoPAP to 8:2 FTOH. While loss of viable bacteria content can occur under aerobic conditions [58,59], rapid freezing to -80 °C or refrigerated fecal storage immediately

following sample collection will not significantly alter bacterial composition if used within an hour [59,60,61].

For the rat fecal assay, the 8:2 monoPAP stock solution was prepared in methanol (5 mg/mL) and the working stock was diluted in water such that the final concentration of methanol was ≤0.1% of the total incubation volume. The fecal supernatant was diluted to 50 mg/mL with phosphate buffer (0.1 M, pH 7.4) in 1.5 mL microcentrifuge tubes, warmed to 37°C, and preheated for 5 minutes. Reactions were initiated with 8:2 monoPAP (concentrations ranging between 400 – 7000 nM) and incubated up to 50 mins (0, 20, 30, 40, and 50 min time points). The final reaction volume was 500 µL. Reactions were terminated with 500 µL ethyl acetate containing 1 µM of the 9ME 8:2 FTOH internal standard, vortexed for 10 minutes, and centrifuged at 10000 rpm for 10 minutes at room temperature. The ethyl acetate layer was removed from the aqueous layer, transferred to a amber glass GC-MS vial, sealed and stored at -20 °C until GC-MS analysis.

Incubation of 8:2 monoPAP in human fecal samples was performed in a vinyl anaerobic chamber maintained at 37°C (5% H_2/95% N_2) from Coy Laboratory Products. The 8:2 monoPAP stock solution was prepared in methanol (5 mg/mL) and the working stock was diluted in water such that the final concentration of methanol was ≤0.1%. The fecal supernatant was diluted to 50 mg/mL with phosphate buffer (0.1 M, pH 7.4) in 1.5 mL microcentrifuge tubes, warmed to 37 °C, and preheated for 5 minutes. The reactions were initiated with 8:2 monoPAP (concentrations ranging between 400 – 7000 nM) and incubated up to 60 minutes (0, 45, 50, 55, and 60 minute time points) to ensure 8:2 FTOH peak signals were quantifiable. The final reaction volume was 500 µL. Reactions were terminated with 500 µL ethyl acetate containing 1 µM of the 9ME 8:2 FTOH internal standard, vortexed for 10 minutes, and centrifuged at 10000 rpm for 10 minutes at room temperature. The ethyl acetate layer was removed from

526 the aqueous layer, transferred to an amber glass GC-MS vial, sealed and stored at -20 °C until GC-MS
527 analysis.

528 *2.5 GC-MS analysis*

529 The GC-MS method was obtained from Lahey et al. [62]. Extracted ethyl acetate layers were
530 analyzed using an Agilent 6890A gas chromatograph coupled with an Agilent 5973 mass spectrometer
531 operating in EI mode. An Agilent J&W HP-5 GC column (30 m x 0.25 mm x 0.25 µm) was used. The
532 GC inlet had an injection temperature of 240 °C, operating in spitless mode, an average velocity flow of
533 25 cm/s, and a high-pressure injection of 1.5 psi. The column temperature program was as follows: 60
534 °C (2 min) → (ramp 10 °C/min) to 120 °C → (ramp 50 °C/min) to 250 °C (3min). The MS had an ion
535 source temperature and interface temperature of 200 °C and 150 °C respectively. The 8:2 FTOH and
536 9ME 8:2 FTOH internal standard were monitored in SIM mode with 463 and 131 m/z (Figure 2.1). The
537 131 m/z was used to quantify both 8:2 FTOH and 9ME 8:2 FTOH internal standard, while 463 m/z was
538 used for 8:2 FTOH peak referencing.

539

540

541

542

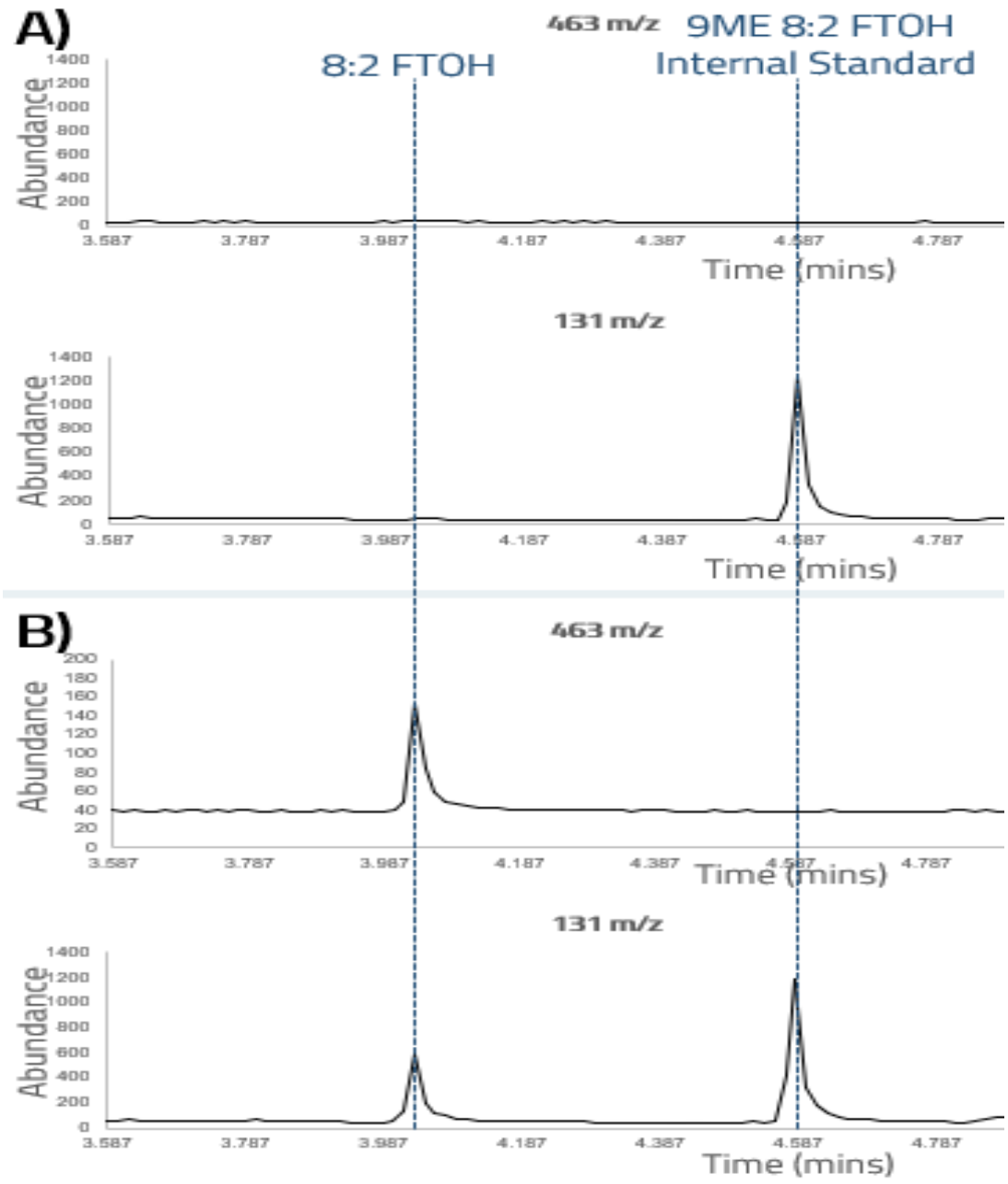

543

544 **Figure 2.1:** GC-MS chromatograms of 8:2 FTOH and 9ME 8:2 FTOH internal standard in **A)** active rat
545 fecal suspensions spiked with 0 nM 8:2 FTOH and 1000 nM 9ME 8:2 FTOH **B)** inactivated rat fecal
546 suspensions spiked with 1000 nM of 8:2 FTOH and 1000 nM 9ME 8:2 FTOH. All analytes were
547 monitored at 463 m/z and 131 m/z.

548

549 *2.6 Bicinchoninic acid (BCA) assay*

550 Rat and human fecal protein concentrations were determined using a BCA assay kit, following
551 instructions as described by the manufacturer. Briefly, 25 µL of bovine serum albumin (BSA) standards
552 and fecal supernatant (N = 1) were each pipetted into wells in a 96-well plate. The BCA working reagent
553 (200 µL) was added to each well and the plate was mixed thoroughly for 30 seconds on a platform
554 shaker. To maintain temperature, the 96-well plate was covered and incubated at 37°C for 30 minutes.
555 The plate was cooled to room temperature and measured at an absorbance of 563 nm on a Molecular
556 Devices SpectraMax 340 PC 384 Microplate Reader. Protein concentrations were determined by
557 comparing the absorption response with respect to the BSA standards. The actual protein concentration
558 was determined to be 30 ± 7 mg/mL and 37 ± 3 mg/mL for the rat and human fecal samples,
559 respectively and were normalized in all subsequent analyses.

560 *2.7 Quality control and data analysis*

561 All samples were collected in triplicate from at least 6 different experiments to generate enzyme
562 kinetic values. The instrumental LOD and LOQ were calculated by 3*(SD/m) and 10*(SD/m)
563 respectively, where SD is the standard deviation and m is the slope of the regression line [63] (Table S1).
564 The relative recovery of 8:2 FTOH in extracted S9 fractions and fecal samples was also determined by
565 spiking 8:2 FTOH (500 or 1000 nM) in heat-inactivated S9 fractions (65°C for 30 minutes) and fecal
566 samples (100°C for 60 minutes). Mean recoveries from triplicate analysis ranged from 60-100% and can
567 be found in Table S1. Analyte responses were not corrected for recovery. To determine the contribution
568 of abiotic, non-enzymatic hydrolysis, heat-inactivated S9 fractions and fecal samples were spiked with
569 the highest 8:2 monoPAP concentration, and incubated at 37 °C for the longest time within each set of
570 experiment. No abiotic hydrolysis was observed in any of the enzyme assays, indicating that the

formation of 8:2 FTOH was due to enzymatically mediated transformation in all samples. Data analysis and statistical comparisons were performed using Systat Software SigmaPlot Version 14. Multiple comparisons were done using one-way ANOVA coupled with the Holm-Sidak method.

3.0 Results and Discussion

3.1 Biotransformation rates of 8:2 monoPAP in rat & human liver, intestine, and feces

The biotransformation of 8:2 monoPAP has been previously demonstrated in mammals both *in vivo* in the rat [16,17] and using purified commercial bovine intestinal phosphatase [24]. In our study, we noted that the 8:2 monoPAP was metabolized rapidly, with 8:2 FTOH production first observed as early as 0.5 minutes in the rat and human liver and intestine (Figure 3.1). These results were similar to the findings of Butt et al. [55] and Jackson and Mabury. [24]. Butt et al. used a similar precursor to 8:2 monoPAP, the 8:2 fluorotelomer acrylate, which hydrolyzed to form 8:2 FTOH in rainbow trout liver and stomach S9 as early as 0.50−1.0 minutes [55]. Jackson and Mabury reported that extrahepatic metabolism in the digestive system was capable of hydrolyzing 8:2 monoPAP in 1.5 minutes [24]. In feces, we observed 8:2 FTOH metabolite formation as early as 20 minutes but cannot eliminate the possibility of 8:2 FTOH formation in shorter time periods as LOD and LOQ were limiting factors in detecting earlier time points.

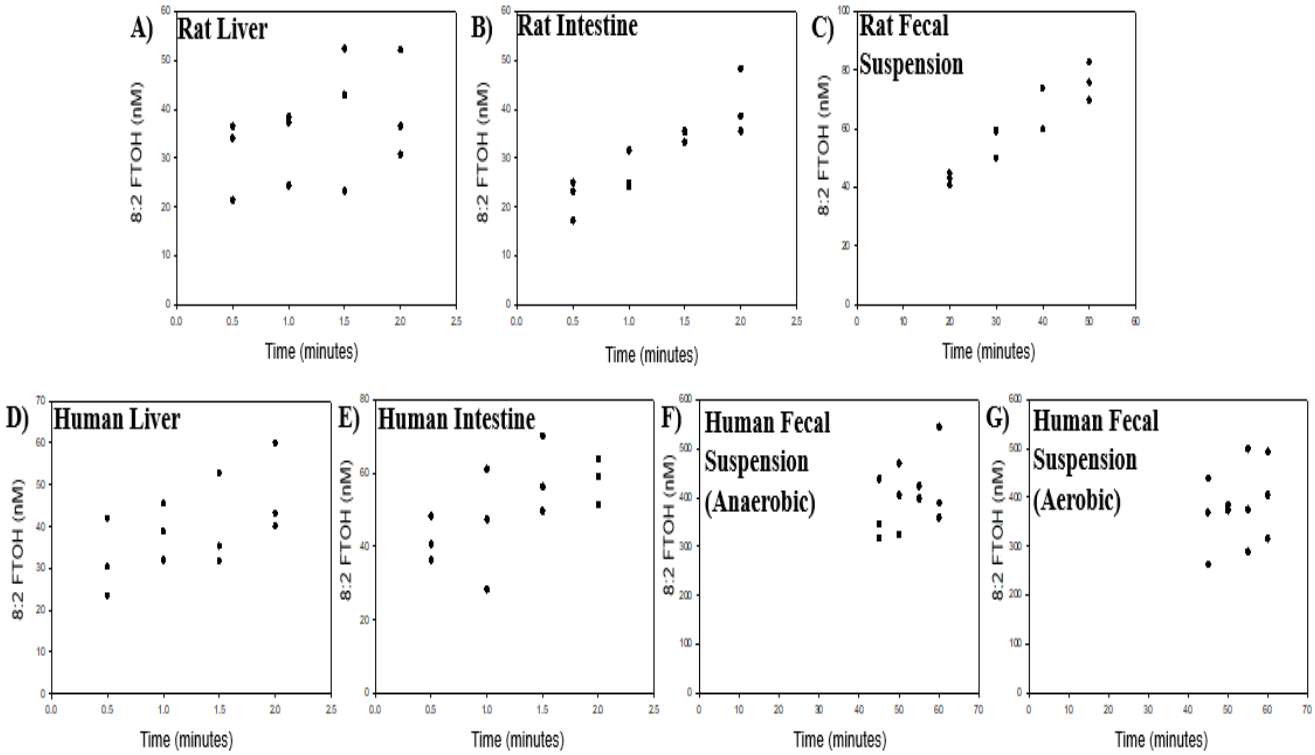

Figure 3.1: Representation of the concentration of 8:2 FTOH formation versus time via incubation of 750 nM 8:2 monoPAP in **A)** rat liver S9 fraction **B)** rat intestinal S9 fraction **C)** rat fecal suspension **D)** human liver S9 fraction **E)** human intestinal S9 fraction **F)** human fecal suspension (anaerobic) **G)** human fecal suspension (aerobic). All concentration time points were performed in triplicates (n = 3) and the biotransformation rate was determined by plotting a regression line against the mean of each concentration time points.

3.2 Interpretation of the Michaelis Menten kinetics between rat and human liver and intestine

Michaelis Menten kinetics plots of 8:2 monoPAP biotransformation in rat and human liver, intestine, and feces are presented in Figure 3.2. To generate the points in the Michalis Menten kinetics plot, formation of 8:2 FTOH versus time with the incubation of various 8:2 monoPAP concentrations was plotted and can be found in Table S2−S8. Nonlinear regression analysis was plotted against the concentration points in each Michaelis Menten kinetics graph, and the V_{max} and K_M values were calculated. From the Michaelis Menten kinetics plots, the associated V_{max} and K_M values are listed in Table 3.1.

A low K_M value indicates a low substrate concentration is needed to form a product as there is a high binding affinity between the substrate and enzyme to form the enzyme substrate complex [53]. Conversely, a high K_M value indicates a high substrate concentration is needed to form a product as there is a low binding affinity between the substate and enzyme to form the enzyme substrate complex [53]. In addition to this fundamental concept, kinetic parameters of low K_M and high V_{max} in an organ is indicative as the major site of metabolism, given its high metabolic efficiency for that substrate [64]. For example, Poet et al. demonstrated that two organophosphate pesticides, Chlorpyrifos and Diazinon, could be metabolized in rat liver and intestinal microsomes where the liver compartment had lower K_M and higher V_{max} compared to the intestine, resulting in a higher metabolic efficiency [64]. In this study, the rat and human intestinal fractions had approximately 2-fold lower K_M values compared to the liver fractions, despite having similar V_{max} values. Despite the similar Vmax, the smaller K_M values in intestine suggest that the intestine has a slightly higher metabolic efficiency and might be the primary target organ for 8:2 monoPAP metabolism, followed by the liver. Theses results may be due to the increased microvilli surface area allowing greater absorptive and metabolic capabilities [64], and also supports the postulation by Jackson et al., that the small intestine contains high number of hydrolytic

638 enzymes (ie. alkaline phosphatase enzymes) that are able to efficiently metabolize 8:2 monoPAP [24].
639 Furthermore, the liver and intestine K_M and V_{max} values were not significantly different between rat and
640 human, indicating the target organ specificity for 8:2 monoPAP was species independent. In contrast,
641 K_M and V_{max} values between rat and human microbiome were notably different. To better compare this
642 potential species difference, as well as the differences between microbiome-mediated versus host
643 biotransformation, we used CL_{Intr} values, which is described in the next section.

644

645

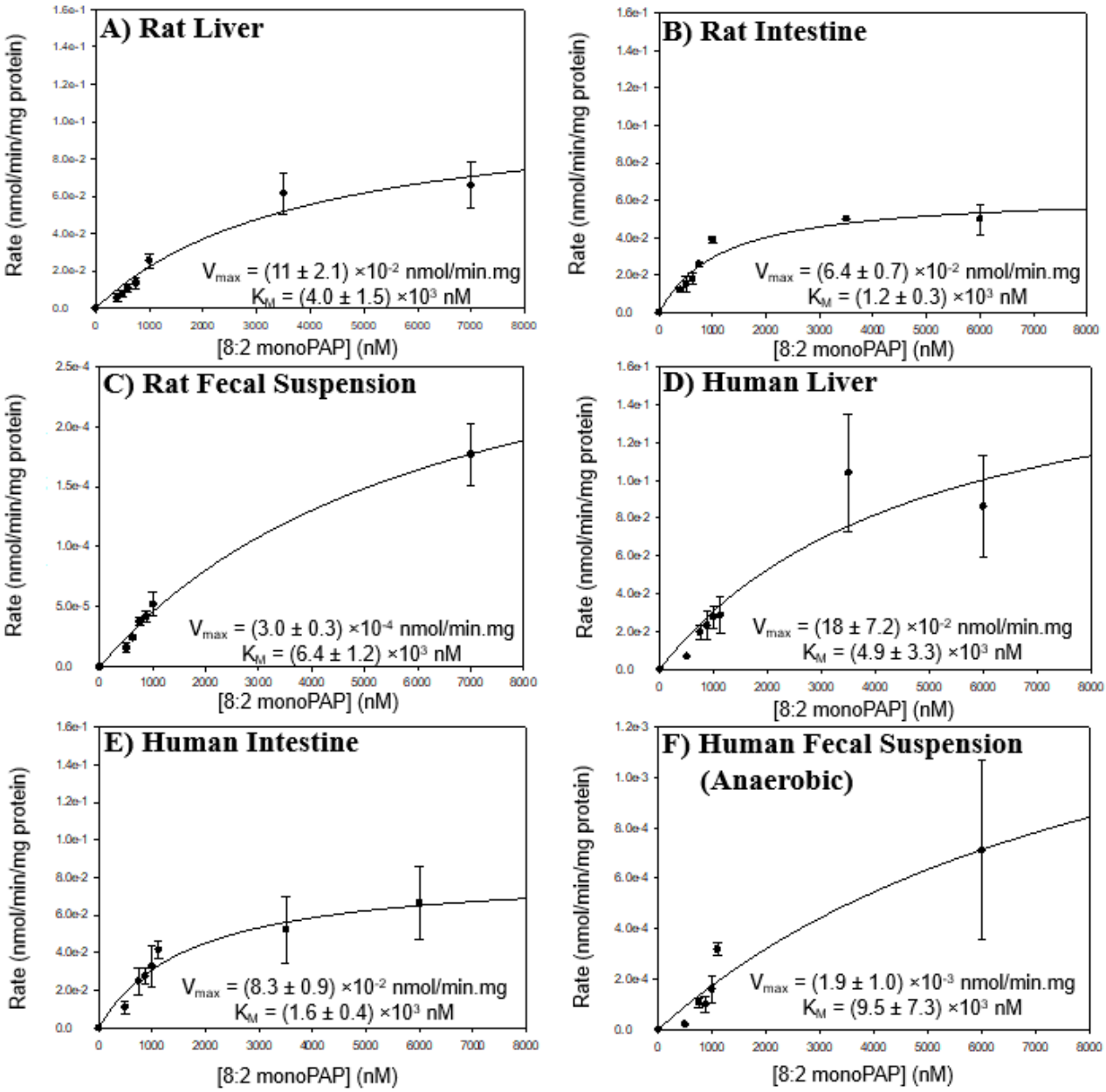

646

647 **Figure 3.2**: Steady-state hydrolysis of 8:2 monoPAP in rat and human liver (A,B), intestine (C,D), and
648 feces (E,F). For reactions, 0.5 mg/mL of S9 or 37 mg/mL fecal suspension, and 8:2 monoPAP (varied
649 from 100-7000 nM) was incubated in phosphate buffer (0.1 mM) at 37 C at pH 7.4. Michaelis constant
650 (KM) and maximum reaction rate (Vmax) was obtained from nonlinear regression analysis. Reported
651 values represent the mean average from three experimental replicates ± standard error.

Table 3.1: Associated V_{max}, K_M, and CL_{Intr} values for the different rat and human fractions. Errors are reported in ± standard error.

	V_{max} (nmol/min.mg)	**K_M (nM)**	**CL_{Intr} (mL/min.mg)**
Rat Liver	$(11 \pm 2.1) \times 10^{-2}$	$(4.0 \pm 1.5) \times 10^{3}$	$(2.8 \pm 1.6) \times 10^{-2}$
Rat Intestine	$(6.4 \pm 0.7) \times 10^{-2}$	$(1.2 \pm 0.3) \times 10^{3}$	$(5.5 \pm 1.7) \times 10^{-2}$
Rat Feces	$(3.0 \pm 0.3) \times 10^{-4}$	$(6.4 \pm 1.2) \times 10^{3}$	$(4.7 \pm 0.6) \times 10^{-5}$
Human Liver	$(18 \pm 7.2) \times 10^{-2}$	$(4.9 \pm 3.3) \times 10^{3}$	$(3.7 \pm 2.9) \times 10^{-2}$
Human Intestine	$(8.3 \pm 0.9) \times 10^{-2}$	$(1.6 \pm 0.4) \times 10^{3}$	$(4.9 \pm 1.3) \times 10^{-2}$
Human Feces (Anaerobic)	$(1.9 \pm 1.0) \times 10^{-3}$	$(9.5 \pm 7.3) \times 10^{3}$	$(2.0 \pm 1.9) \times 10^{-4}$
Human Feces (Aerobic)	$(2.9 \pm 1.9) \times 10^{-3}$	$(2.1 \pm 1.7) \times 10^{4}$	$(1.4 \pm 1.5) \times 10^{-4}$

Comparison of intrinsic clearance levels

For *in vivo* studies, the clearance of a drug or toxicant can only be determined through renal excretion or blood concentration and therefore, *in vitro* clearance prediction is needed to determine clearance from other organs such as the liver [65]. The use of intrinsic clearance levels (CL_{Intr}) is used to measure the total enzyme activities in the organ that are responsible for metabolism [54,65], and excludes physiological factors such as blood flow and drug/toxin binding abilities [65]. In this study, the CL_{Intr} values for rat and human liver, intestine, and feces are shown in Table 3.1 and Figure 3.3. The CL_{Intr} for each fraction was calculated by dividing the V_{max} by K_M value [54,65]. The CL_{Intr} was not statistically different in the rat intestine compared to the rat liver. For the human model, the same trend was observed. This suggests that there are high levels of hydrolytic enzymes (e.g. alkaline phosphatase enzymes) found in the small intestine mucosa and the liver, responsible for transformation of 8:2

666 monoPAP and supports the findings by Jackson et al [24]. After oral exposure to 8:2 monoPAP, the GI
667 tract is the first site of possible metabolism [17], we predict that most of the 8:2 monoPAP transformation
668 occurs within the intestinal tract, before reaching the liver for further transformation.. In addition, the
669 CL_{Intr} ratios between the rat and human intestine and liver were not statistically significant, suggesting
670 that there were limited species differences. Overall, these results were consistent with the findings
671 reported by D'eon et al., which hypothesized monoPAP to be metabolized to FTOH in the gut, followed
672 by absorption of FTOH into the bloodstream for further transformation [17].

673 The rat microbiome contribution to 8:2 monoPAP transformation was approximately 600-fold
674 and 1100-fold less than the rat liver and intestine respectively. The human microbiome contribution to
675 8:2 monoPAP transformation was 200-fold and 250-fold less than the human liver and intestine
676 respectively. Together, these results demonstrate that fecal bacteria play less of a role in clearing the
677 monoPAP from systemic circulation. This might be because the liver and intestine are the primary sites
678 for 8:2 monoPAP metabolism while the fecal microbes in the lower GI tract are passive contributors.
679 Microbial diversity in these feces collected from individuals may also impact the CL_{Intr} of 8:2 monoPAP,
680 given that diet, environment, and genetics factors could alter the number of active microbes [66,67],
681 possibly altering the ability to metabolize these PFAS compounds.

682 When comparing between human fecal incubation conditions, CL_{Intr} in anaerobic condition was
683 no different compared to those from the aerobic conditions, supporting other studies that demonstrated
684 the viability of bacteria when stored at -20 °C and used in an 1-hour assay at 37 °C [56,59,60,61]. Given that
685 these fecal microbes are found in highly anaerobic regions of the lower GI tract [56] and were stripped out
686 of their natural environment, the CL_{Intr} may be greater in anaerobic conditions during a longer time
687 course (i.e. > 1 hour) compared to aerobic conditions as more active functional microbes will be able to

688 metabolize these 8:2 monoPAP. This has been shown by others, where loss of viable anaerobic bacteria
689 occurs in collected fecal samples over time [58,61].
690
691
692
693
694
695

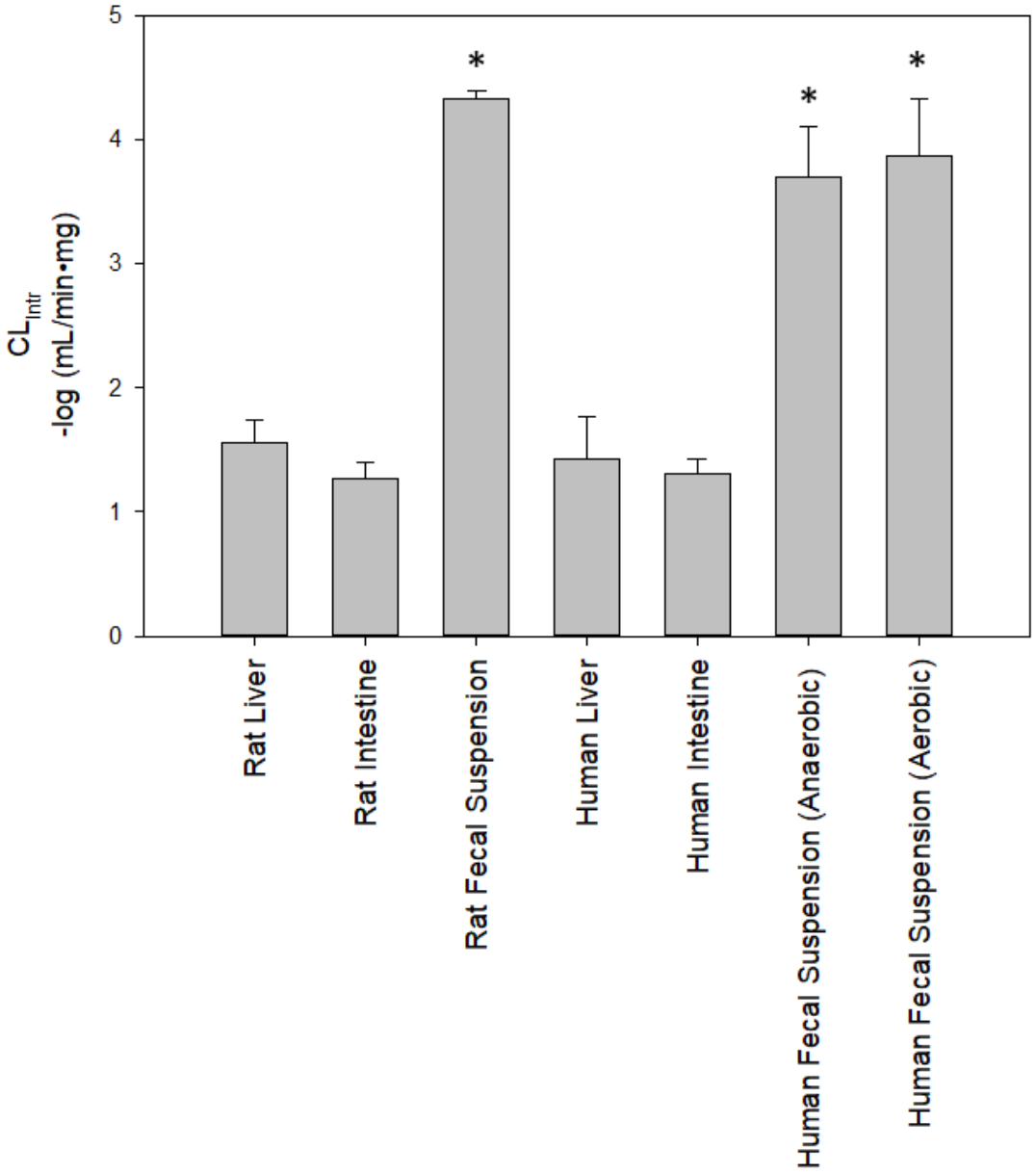

696

697 **Figure 3.3:** Comparison of clearance level intrinsic (CL_{Intr}) between rat and human liver, intestine, and
698 feces, calculated from Systat Software SigmaPlot Version 14 using one-way ANOVA with Holm-Sidak
699 method ($p<0.05$). *Denotes significant clearance level intrinsic differences between that versus rat and
700 human liver and intestine. Error bars are reported as ± standard error.

701

Limitations and future outlooks

In this present study, we have monitored the metabolism of 8:2 monoPAP to 8:2 FTOH with the use of GC-MS. While many published studies report product formation as a method to calculate kinetics, monitoring both the depletion of 8:2 monoPAP with LC-MS/MS alongside the formation of 8:2 FTOH would provide additional information regarding substrate fate and transformation. Monitoring 8:2 monoPAP loss with 8:2 FTOH formation would allow us to understand the total mass balance of the reaction, establishing the fraction of 8:2 monoPAP transforming to 8:2 FTOH, compared to the unreacted fraction, whether there may be other products, and/or 8:2 monoPAP loss due to adsorption onto the plastic vial.

We have also demonstrated the fecal microbes have the capability of metabolising 8:2 monoPAP to 8:2 FTOH. With the diversity of microbial species [42], further investigation is needed to identify the specific bacteria or bacterial enzyme responsible for these 8:2 monoPAP transformations. For example, Zimmermann et al. have looked at the drugs containing ester group functionalities and determined Bacteroidetes in human microbiome to be a contributor in this metabolic pathway [51]. Furthermore, Poet et al. showed that A-esterase (PON1) found in enterocytes can metabolize ester containing drugs Chlorpyrifos and Diazinon to trichloropyridinol and 2-isopropyl-4-methyl-6-hydroxypyrimidine [64]. The use of antibiotics has been shown to alter the microbiota functions by killing or inhibiting their mechanisms [68]. Using these antibiotics, we can select specific antibiotics to target bacteria or bacterial enzymes of interest that are contributing to 8:2 monoPAP metabolism.

With the diverse microbial species in the large intestine [42], future experiments should be conducted to examine whether 8:2 monoPAP can yield downstream carboxylic acid metabolites, including the 8:2 FTCA, 8:2 FTUCA and PFOA (Figure 3.4). Lee et al. and Zhang et al. both observed

724 metabolite products of 8:2 FTCA, 8:2 FTUCA, and PFOA in WWTP sludge from the biodegradation
725 from 8:2 monoPAP and 8:2 FTOH respectively [22,69]. Zhang et al. also reported higher levels of 8:2
726 FTCA than 8:2 FTUCA and PFOA [64] while Lee et al. noted longer chain PAPs (i.e. 8:2−10:2 monoPAP)
727 had degradation stop at 8:2 FTCA and 8:2 FTUCA [19], and is possibly due to the increased steric
728 hinderance of these longer chained compounds that are resistant to further degradation [19]. This is
729 important since 8:2 FTCA and 8:2 FTUCA can be several orders of magnitude more toxic than PFOA [70].
730 Given these WWTP microbial studies as well as the variety of possible xenobiotic biotransformation
731 mechanisms the human microbiome is capable of (i.e. hydrolysis [43–45], nitro-reduction [45,46],
732 hydroxylation [45,47], and methylation [45,48]), we suspect that microbes in the human GI can perform similar
733 monoPAP transformations, yielding fluorotelomer acids (i.e. FTCAs, FTUCAs) and perfluorinated acids
734 (i.e. PFCAs).

735 Lastly, this study looks at the fecal microbiome transformation of a long chain polyfluoroalkyl
736 phosphate ester compound, the 8:2 monoPAP. As industries phased out longer chain PFAS and moved
737 towards short chain PFAS compounds [27], future investigation should look at the biotransformation of
738 shorter chain 4:2−6:2 monoPAPs as they will be more relevant to the industry. In addition, the
739 metabolism of different chain length diPAP and triPAP should also be investigated. As Lee et al and
740 D'eon et al. reported that the half life of PAPs increase with increase chain legnth [17,22], we predict that
741 the rate of FTOH formation in fecal microbiome will be greater for shorter chain PAPs compared to
742 longer chain PAP.

743

744

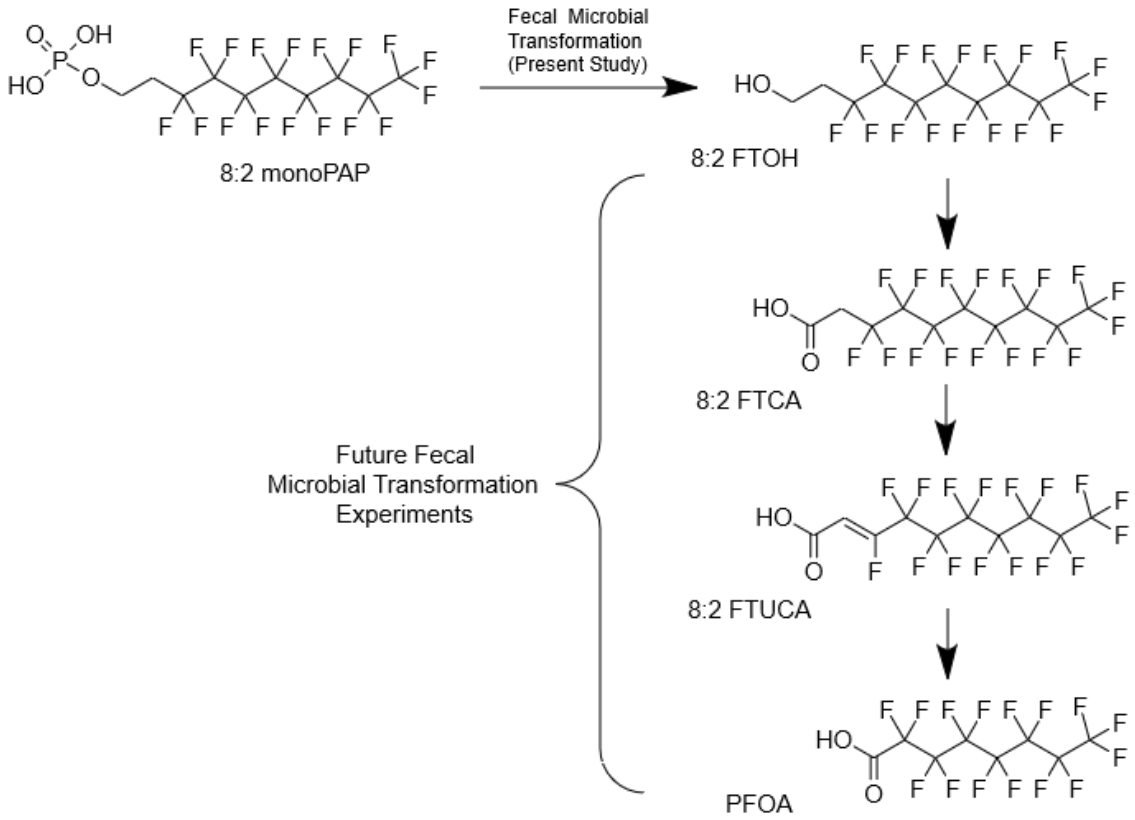

745

746 **Figure 3.4:** Fecal microbial transformation of 8:2 monoPAP precursor to other carboxylic acid products.

747

748

749

750

751

752

753

4.0 Conclusion

In conclusion, our current study illustrates that 8:2 monoPAP can be metabolized in the liver, intestine, and by fecal microbes in rats and humans. This is the first study to demonstrate that the rat and human microbiome are contributors in metabolizing 8:2 monoPAP and should not be overlooked, even if the liver and intestine are the predominate organs for metabolism and detoxification. We reported that the metabolism of 8:2 monoPAP to 8:2 FTOH in intestine was approximately similar to the liver in rat and human. However, metabolism in rat and human feces were significantly lower compared to the liver and intestine. This suggests that fecal bacteria in the GI tract play a reduced role in monoPAP metabolism.

In future studies, experiments should examine the possibilities of fecal microbiome metabolism of 8:2 monoPAP (or other short chain PFAS) to other transformation products, given the diversified strains of microbial species. We are currently conducting a collaborative study with Dr. Alex Wong (Department of Biology, Carleton University) to identify the bacteria present within the pooled human fecal sample, to shed light on those bacteria potentially responsible for PFAS transformation. In addition, future experiments should look at the metabolism of shorter chain 4:2−6:2 monoPAPs and the di/triPAP will be more industrial relevant.

References

1. Buck, R. C. *et al.* Perfluoroalkyl and polyfluoroalkyl substances in the environment: Terminology, classification, and origins. *Integr. Environ. Assess. Manag.* 7(4):513-41 (2011) doi:10.1002/ieam.258.

2. Kissa, E. Fluorinated Surfactants and Repellents: Second Edition, Revised and Expanded Surfactant Science Series. *J. Am. Chem. Soc.* 97:80-102 (2001) doi:10.1021/ja015260a.

3. Daly, E. R. *et al.* Per- and polyfluoroalkyl substance (PFAS) exposure assessment in a community exposed to contaminated drinking water, New Hampshire, 2015. *Int. J. Hyg. Environ. Health.* 221(3):569-577 (2018) doi:10.1016/j.ijheh.2018.02.007.

4. Yan, H. *et al.* Short- and long-chain perfluorinated acids in sewage sludge from Shanghai, China. *Chemosphere.* 88(11):1300-1305 (2012) doi:10.1016/j.chemosphere.2012.03.105.

5. Eriksson, U. & Kärrman, A. World-Wide Indoor Exposure to Polyfluoroalkyl Phosphate Esters (PAPs) and other PFASs in Household Dust. *Environ. Sci. Technol.* 49(24):14503-14511 (2015) doi:10.1021/acs.est.5b00679.

6. Worley, R. R. *et al.* Per- and polyfluoroalkyl substances in human serum and urine samples from a residentially exposed community. *Environ. Int.* 106:135-143 (2017) doi:10.1016/j.envint.2017.06.007.

7. OECD. Toward a new comprehensive global database of per- and polyfluoroalkyl substances (PFASs): Summary Report on Updating the OECD 2007 List of Per- and Polyfluoroalkyl Substances (PFASs). *Series on Risk Management* (2018).

8. Zhang, W. *et al*. Exposure of Juncus effusus to seven perfluoroalkyl acids: Uptake, accumulation

and phytotoxicity. *Chemosphere.* 233:300-308 (2019) doi:10.1016/j.chemosphere.2019.05.258.

9. Åkerblom, S. *et al*. Variation and accumulation patterns of poly- and perfluoroalkyl substances (PFAS) in European perch (Perca fluviatilis) across a gradient of pristine Swedish lakes. *Sci. Total Environ.* 599-600: 1685-1692 (2017) doi:10.1016/j.scitotenv.2017.05.032.

10. Pérez, F. *et al.* Accumulation of perfluoroalkyl substances in human tissues. *Environ. Int.* 59:354-362 (2013) doi:10.1016/j.envint.2013.06.004.

11. Conder, J. M. *et al.* Are PFCAs bioaccumulative? A critical review and comparison with regulatory criteria and persistent lipophilic compounds. *Environ. Sci. Technol.* 42(4):995-1003 (2008) doi:10.1021/es070895g.

12. Butt, C. M. *et al*. Biotransformation pathways of fluorotelomer-based polyfluoroalkyl substances: A review. *Environ. Toxicol. Chem.* 33(2):243-67 (2014) doi:10.1002/etc.2407.

13. Gebbink, W. A. *et al*. Polyfluoroalkyl phosphate esters and perfluoroalkyl carboxylic acids in target food samples and packaging-method development and screening. *Environ. Sci. Pollut. Res.* 20(11):7949-58 (2013) doi:10.1007/s11356-013-1596-y.

14. Schaider, L. A. *et al.* Fluorinated Compounds in U.S. Fast Food Packaging. *Environ. Sci. Technol. Lett.* 4(3):105-111 (2017) doi:10.1021/acs.estlett.6b00435.

15. Trier, X. *et al*. Structural isomers of polyfluorinated di- and tri-alkylated phosphate ester surfactants present in industrial blends and in microwave popcorn bags. *Environ. Sci. Pollut. Res.* 18:1422-1432 (2011) doi:10.1007/s11356-011-0488-2.

16. D'Eon, J. C. & Mabury, S. A. Production of perfluorinated carboxylic acids (PFCAs) from the biotransformation of polyfluoroalkyl phosphate surfactants (PAPS): Exploring routes of human

contamination. *Environ. Sci. Technol.* 41(13):4799-805 (2007) doi:10.1021/es070126x.

17. D'eon, J. C. & Mabury, S. A. Exploring indirect sources of human exposure to perfluoroalkyl carboxylates (PFCAs): Evaluating uptake, elimination, and biotransformation of polyfluoroalkyl phosphate esters (PAPs) in the Rat. *Environ. Health Perspect.* 19(3): 344–350 (2011) doi:10.1289/ehp.1002409.

18. Poothong, S. *et al*. Distribution of Novel and Well-Known Poly- and Perfluoroalkyl Substances (PFASs) in Human Serum, Plasma, and Whole Blood. *Environ. Sci. Technol.* 51(22):13388-13396 (2017) doi:10.1021/acs.est.7b03299.

19. Begley, T. H. *et al*. Migration of fluorochemical paper additives from food-contact paper into foods and food simulants. *Food Addit. Contam. - Part A Chem. Anal. Control. Expo. Risk Assess.* 25(3):384-90 (2008) doi:10.1080/02652030701513784.

20. Ebnesajjad, S. Fluoroplastics, Volume 1 - Non-Melt Processible Fluoropolymers - The Definitive User's Guide and Data Book (2nd Edition). *Fluoroplastics*, *Elsevier Science & Technology Books.* 1:27-37 (2014). doi:10.1016/C2012-0-05997-2.

21. Harrad, S. Persistent Organic Pollutants. *Blackwell Publishing Ltd.* 25-69 (2009). doi:10.1002/9780470684122.

22. Lee, H. *et al*. Biodegradation of polyfluoroalkyl phosphates as a source of perfluorinated acids to the environment. *Environ. Sci. Technol.* 44(9):3305-3310 (2010) doi:10.1021/es9028183.

23. Zabaleta, I. *et al.* Biotransformation of 8:2 polyfluoroalkyl phosphate diester in gilthead bream (Sparus aurata). *Sci. Total Environ.* 609:1085-1092 (2017) doi:10.1016/j.scitotenv.2017.07.241.

24. Jackson, D. A. & Mabury, S. A. Enzymatic kinetic parameters for polyfluorinated alkyl phosphate

hydrolysis by alkaline phosphatase. *Environ. Toxicol. Chem.* 31(9):1966-71 (2012) doi:10.1002/etc.1922.

25. Martin, J. W. *et al*. Dietary accumulation of perfluorinated acids in juvenile rainbow trout (Oncorhynchus mykiss). *Environ. Toxicol. Chem.* 22(1):189-95 (2003) doi:10.1897/1551-5028(2003)022<0189:daopai>2.0.co;2.

26. Martin, J. W. *et al.* Bioconcentration and tissue distribution of perfluorinated acids in rainbow trout (Oncorhynchus mykiss). *Environ. Toxicol. Chem.* 22(1):196-204 (2003) doi:10.1897/1551-5028(2003)022<0196:batdop>2.0.co;2.

27. Ritter, S. K. Fluorochemicals go short. *Chem. Eng. News.* 88(5):12-17 (2010) doi:10.1021/cen-v088n005.p012.

28. Temkin, A. M. *et al*. Application of the key characteristics of carcinogens to per and polyfluoroalkyl substances. *Int. J. Environ. Res. Public Health.* 17(5):1668 (2020) doi:10.3390/ijerph17051668.

29. Huang, M. C. *et al.* Toxicokinetics of perfluorobutane sulfonate (PFBS), perfluorohexane-1-sulphonic acid (PFHxS), and perfluorooctane sulfonic acid (PFOS) in male and female Hsd:Sprague Dawley SD rats after intravenous and gavage administration. *Toxicol. Reports.* 6:645-655 (2019) doi:10.1016/j.toxrep.2019.06.016.

30. Dzierlenga, A. L. *et al.* Toxicokinetics of perfluorohexanoic acid (PFHxA), perfluorooctanoic acid (PFOA) and perfluorodecanoic acid (PFDA) in male and female Hsd:Sprague dawley SD rats following intravenous or gavage administration. *Xenobiotica.* 50(6):722-732 (2020) doi:10.1080/00498254.2019.1683776.

31. Olsen, G. W. *et al.* Half-life of serum elimination of perfluorooctanesulfonate, perfluorohexanesulfonate, and perfluorooctanoate in retired fluorochemical production workers. *Environ. Health Perspect.* 115(9):1298-305 (2007) doi:10.1289/ehp.10009.

32. Huang, M. C. *et al.* Toxicokinetics of 8:2 fluorotelomer alcohol (8:2-FTOH) in male and female Hsd:Sprague Dawley SD rats after intravenous and gavage administration. *Toxicol. Reports.* 6:924-932 (2019) doi:10.1016/j.toxrep.2019.08.009.

33. Chang, S. C. *et al.* Comparative pharmacokinetics of perfluorobutyrate in rats, mice, monkeys, and humans and relevance to human exposure via drinking water. *Toxicol. Sci.* 104(1):40-53 (2008) doi:10.1093/toxsci/kfn057.

34. Russell, M. H. *et al.* Elimination kinetics of perfluorohexanoic acid in humans and comparison with mouse, rat and monkey. *Chemosphere.* 93(10):2419-2425 (2013) doi:10.1016/j.chemosphere.2013.08.060.

35. Jia, L. & Liu, X. The Conduct of Drug Metabolism Studies Considered Good Practice (II): *In Vitro* Experiments. *Curr. Drug Metab.* 8(8):822-829 (2007) doi:10.2174/138920007782798207.

36. Richardson, J. S. *et al*. Efficiency in Drug Discovery: Liver S9 Fraction Assay As a Screen for Metabolic Stability. *Drug Metab. Lett.* 10(2):83-90 (2016) doi:10.2174/1872312810666160223121836.

37. Nishimuta, H. *et al*. Hepatic, intestinal, renal, and plasma hydrolysis of prodrugs in human, cynomolgus monkey, dog, and rat: Implications for in vitro-in vivo extrapolation of clearance of prodrugs. *Drug Metab. Dispos.* 2(9):1522-1531 (2014) doi:10.1124/dmd.114.057372.

38. Von Richter, O. *et al.* Determination of in vivo absorption, metabolism, and transport of drugs by

the human intestinal wall and liver with a novel perfusion technique. *Clin. Pharmacol. Ther.* 70(3):217-227 (2001) doi:10.1067/mcp.2001.117937.

39. Fritz, A. *et al.* Expression of clinically relevant drug-metabolizing enzymes along the human intestine and their correlation to drug transporters and nuclear receptors: An intra-subject analysis. *Basic Clin. Pharmacol. Toxicol.* 124(3):245-255 (2019) doi:10.1111/bcpt.13137.

40. Smith, D. A. *et al*. Clearance in Drug Design. *J. Med. Chem.* 62(5):2245-2255 (2019) doi:10.1021/acs.jmedchem.8b01263.

41. Ionescu, C. & Caira, M. R. Drug metabolism: Current concepts. *Drug Metabolism, Springer Netherlands.* (2005). doi:10.1007-1-4020-4142-x.

42. Rajilić-Stojanović, M. & de Vos, W. M. The first 1000 cultured species of the human gastrointestinal microbiota. *FEMS Microbiol. Rev.* 38(5):996-1047 (2014) doi:10.1111/1574-6976.12075.

43. Gratz, S. W. *et al.* Masked trichothecene and zearalenone mycotoxins withstand digestion and absorption in the upper GI tract but are efficiently hydrolyzed by human gut microbiota in vitro. *Mol. Nutr. Food Res.* 61(4) (2017) doi:10.1002/mnfr.201600680.

44. Dall'Erta, A. *et al.* Masked mycotoxins are efficiently hydrolyzed by human colonic microbiota releasing their aglycones. *Chem. Res. Toxicol.* 26(3):305-312 (2013) doi:10.1021/tx300438c.

45. Claus, S. P. *et al*. The gut microbiota: A major player in the toxicity of environmental pollutants? *npj Biofilms and Microbiomes.* 2:16003 (2016) doi:10.1038/npjbiofilms.2016.3.

46. Rickert, D. E. *et al*. Metabolism and excretion of 2,4-[14C]dinitrotoluene in conventional and axenic Fischer-344 rats. *Toxicol. Appl. Pharmacol.* 64(1):160-168 (1981) doi:10.1016/0041-

008X(81)90312-4.

47. Van de Wiele, T. *et al.* Human colon microbiota transform polycyclic aromatic hydrocarbons to estrogenic metabolites. *Environ. Health Perspect.* 113(1):6-10 (2005) doi:10.1289/ehp.7259.

48. Bakke, J. E. *et al*. Metabolism of 2,4',5-trichlorobiphenyl by the mercapturic acid pathway. *Science.* 2174560):645–647 (1982) doi: 10.1126/science.6806905.

49. Vázquez-Baeza, Y. *et al.* Impacts of the Human Gut Microbiome on Therapeutics. *Annu. Rev. Pharmacol. Toxicol.* 58:253-270 (2018) doi:10.1146/annurev-pharmtox-042017-031849.

50. Swanson, H. I. Drug Metabolism by the Host and Gut Microbiota: A Partnership or Rivalry? *Drug Metab. Dispos.* 43(10):1499-1504 (2015) doi:10.1124/dmd.115.065714.

51. Zimmermann, M. *et al*. Mapping human microbiome drug metabolism by gut bacteria and their genes. *Nature.* 570(7762):462-467 (2019) doi:10.1038/s41586-019-1291-3.

52. Liu, W. Introduction to Modeling Biological Cellular Control Systems (1st ed. 2012). *Springer Milan.* (2012). doi:10.1007/978-88-470-2490-8.

53. Berg, J. *et al*. Biochemistry, 5. *Auflage*. *New York: W H Freeman* (2002).

54. Rane, A. *et al*. Prediction of hepatic extraction ratio from *in vitro* measurement of intrinsic clearance. *J. Pharmacol. Exp. Ther.* 200(2):420-424 (1977).

55. Butt, C. M. *et al*. Biotransformation of the 8:2 fluorotelomer acrylate in rainbow trout. 2. *In vitro* incubations with liver and stomach S9 fractions. *Environ. Toxicol. Chem.* 29(12):2736-41 (2010) doi:10.1002/etc.348.

56. Davis, C. P. Medical Microbiology. 4th edition. Chapter 6 Normal Flora. *Medical Microbiology*

(1996). doi:10.1016/S0749-5978(03)00027-X.

57. McCabe, M. *et al.* Defining the Role of Gut Bacteria in the Metabolism of Deleobuvir: *In Vitro* and In Vivo Studies. *Drug Metab. Dispos.* 43(10):1612-8 (2015) doi:10.1124/dmd.115.064477.

58. Bellali, S. *et al*. Among live and dead bacteria, the optimization of sample collection and processing remains essential in recovering gut microbiota components. *Front. Microbiol.* 10:1606 (2019) doi:10.3389/fmicb.2019.01606.

59. Papanicolas, L. E. *et al.* Bacterial viability in faecal transplants: Which bacteria survive? *EBioMedicine.* 41:509-516 (2019) doi:10.1016/j.ebiom.2019.02.023.

60. Choo, J. M. *et al*. Sample storage conditions significantly influence faecal microbiome profiles. *Sci. Rep.* 5:16350 (2015) doi:10.1038/srep16350.

61. Brusa, T. *et al*. Oxygen tolerance of anaerobic bacteria isolated from human feces. *Curr. Microbiol.* 19:39-43 (1989) doi:10.1007/BF01568901.

62. Lahey, C. M. *et al*. Fast and Accurate Analysis of Fluorotelomer Alcohols and Acrylates using Triple Quadrupole GC-MS / MS ASMS. *Shimadzu.* 1–8 (2016).

63. Ershadi, S. & Shayanfar, A. Are LOD and LOQ reliable parameters for sensitivity evaluation of spectroscopic methods? *J. AOAC Int.* 101(4):1212-1213 (2018) doi:10.5740/jaoacint.17-0363.

64. Poet, T. S. *et al*. *In vitro* rat hepatic and intestinal metabolism of the organophosphate pesticides chlorpyrifos and diazinon. *Toxicol. Sci.* 72(2):193-200 (2003) doi:10.1093/toxsci/kfg035.

65. Gunaratna, C. Drug metabolism and pharmacokinetics in drug discovery: a primer for bioanalytical chemists, part II. *Curr Sep* 19(3):87-92 (2001).

941 66. Wen, L. & Duffy, A. Factors influencing the gut microbiota, inflammation, and type 2 diabetes. *J.*
942 *Nutr.* 147(7):1468S-1475S (2017) doi:10.3945/jn.116.240754.

943 67. Phillips, M. L. Gut reaction: Environmental effects on the human microbiota. *Environ. Health*
944 *Perspect.* 117(5):A198-A205 (2009) doi:10.1289/ehp.117-a198.

945 68. Zhang, S. *et al*. Facing a new challenge: The adverse effects of antibiotics on gut microbiota and
946 host immunity. *Chin. Med. J.* 132(10):1135-1138 (2019) doi:10.1097/CM9.0000000000000245.

947 69. Zhang, S. *et al.* 6:2 and 8:2 fluorotelomer alcohol anaerobic biotransformation in digester sludge
948 from a WWTP under methanogenic conditions. *Environ. Sci. Technol.* 47(9):4227-4235 (2013)
949 doi:10.1021/es4000824.

950 70. Phillips, M. M., Dinglasan-Panlilio, M. J. A., Mabury, S. A., Solomon, K. R. & Sibley, P. K.
951 Fluorotelomer acids are more toxic than perfluorinated acids. *Environ. Sci. Technol.* 41:7159-
952 7163 (2007) doi:10.1021/es070734c.

953

Supplementary Information Data

Table S1. Limit of detection, limit of quantification, and spike and recovery of 8:2 FTOH in heat inactivated rat & human liver S9 fraction, intestine S9 fraction, and fecal suspension.

	Rat Liver	Rat Intestine	Rat Fecal	Human Liver	Human Intestine	Human Fecal (Anaerobic)	Human Fecal (Aerobic)
Instrumental LOD (nM)	**Instrument A** 4					**Instrument B** 75	
Instrumental LOQ (nM)	**Instrument A** 14					**Instrument B** 251	
Percent Recovery (%)	95 ± 12%*	100 ± 10%**	76 ± 5%**	98 ± 5%**	90 ± 15%**	63 ± 6%**	

Note: Limit of detection (LOD), Limit of quantification (LOQ), and nanomolar (nM). *Spiked with 500 nM of 8:2 FTOH and **Spiked with 1000 nM of 8:2 FTOH. Percent recoveries are reported in ± relative standard deviation.

Table S2. Levels of 8:2 FTOH versus time with the incubation of various 8:2 monoPAP concentrations in rat liver S9 fraction.

Concentration of 8:2 monoPAP incubated (nM)	**0.5 min**	**1 min**	**1.5 min**	**2 min**
400	25 ± 1*	24 ± 4*	27 ± 4*	28 ± 1*
500	24 ± 2*	24 ± 1*	27 ± 5*	29 ± 1*
600	24 ± 3*	27 ± 3*	31 ± 7*	32 ± 0.2*
750	30 ± 8*	33 ± 8*	39 ± 14*	39 ± 11*
1000	30 ± 5*	38 ± 3*	46 ± 1*	48 ± 1*
3500	110 ± 23*	116 ± 37*	143 ± 20*	152 ± 19*
7000	372 ± 80*	399 ± 80*	402 ± 88*	426 ± 51*

Note: *Concentration of 8:2 FTOH in nM and errors are reported as ± standard deviation.

Table S3. Levels of 8:2 FTOH versus time with the incubation of various 8:2 monoPAP concentrations in rat intestinal S9 fraction.

Concentration of 8:2 monoPAP incubated (nM)	**0.5 min**	**1 min**	**1.5 min**	**2 min**
400	22 ± 4*	25 ± 6*	27 ± 9*	31 ± 7*
500	28 ± 2*	29 ± 2*	33 ± 1*	40 ± 1*
625	30 ± 2*	34 ± 1*	37 ± 3*	44 ± 1*
750	21 ± 4*	26 ± 4*	34 ± 1*	40 ± 7*
1000	31 ± 3*	39 ± 7*	51 ± 7*	60 ± 5*
3500	80 ± 17*	93 ± 23*	103 ± 31*	118 ± 30*
6000	124 ± 45*	135 ± 23*	155 ± 41*	159 ± 39*

Note: *Concentration of 8:2 FTOH in nM and errors are reported as ± standard deviation.

Table S4. Levels of 8:2 FTOH versus time with the incubation of various 8:2 monoPAP concentrations in rat fecal suspensions (aerobic).

Concentration of 8:2 monoPAP incubated (nM)	**20 min**	**30 min**	**40 min**	**50 min**
500	25 ± 5*	34 ± 4*	38 ± 4*	39 ± 12*
625	31 ± 5*	37 ± 11*	43 ± 7*	53 ± 9*
750	42 ± 2*	56 ± 5*	69 ± 8*	75 ± 6*
875	30 ± 2*	43 ± 9*	59 ± 6*	66 ± 2*
1000	88 ± 7*	91 ± 9*	114 ± 9*	132 ± 3*
7000**	201 ± 20*	210 ± 7*	226 ± 18*	231 ± 20*

Note: * Concentration of 8:2 FTOH in nM and errors are reported as ± standard deviation. **Incubation time for that concentration was 22, 24, 26, and 28 minutes instead of 20, 30, 40, and 50 minutes.

Table S5. Levels of 8:2 FTOH versus time with the incubation of various 8:2 monoPAP concentrations in human liver S9 fraction.

Concentration of 8:2 monoPAP incubated (nM)	**0.5 min**	**1 min**	**1.5 min**	**2 min**
500	16 ± 2*	17 ± 2*	19 ± 4*	21 ± 2*
750	31 ± 9*	38 ± 6*	39 ± 11*	47 ± 10*
875	33 ± 7*	37 ± 5*	49 ± 9*	48 ± 4*
1000	33 ± 6*	39 ± 4*	42 ± 27*	55 ± 5*
1125	35 ± 12*	52 ± 5*	55 ± 13*	58 ± 12*
3500	132 ± 48*	178 ± 27*	171 ± 24*	221 ± 68*
6000	117 ± 47*	151 ± 42*	145 ± 75*	191 ± 51*

Note: * Concentration of 8:2 FTOH in nM and errors are reported as ± standard deviation.

Table S6. Levels of 8:2 FTOH versus time with the incubation of various 8:2 monoPAP concentrations in human intestinal S9 fraction.

Concentration of 8:2 monoPAP incubated (nM)	0.5 min	1 min	1.5 min	2 min
500	23 ± 1*	24 ± 7*	26 ± 7*	32 ± 6*
750	41 ± 6*	45 ± 16*	58 ± 10*	58 ± 6*
875	29 ± 7 *	34 ± 10 *	45 ± 6*	48 ± 8*
1000	23 ± 3*	31 ± 7*	31 ± 5*	50 ± 2*
1125	52 ± 12*	66 ± 26*	77 ± 24*	83 ± 3*
3500	193 ± 46*	217 ± 80*	235 ± 58*	231 ± 33*
6000	218 ± 61*	223 ± 59*	235 ± 28*	270 ± 79*

Note: * Concentration of 8:2 FTOH in nM and errors are reported as ± standard deviation.

Table S7. Levels of 8:2 FTOH versus time with the incubation of various 8:2 monoPAP concentrations in human fecal suspension (anaerobic).

Concentration of 8:2 monoPAP incubated (nM)	**45 min**	**50 min**	**55 min**	**60 min**
500	271 ± 15*	271 ± 22*	276 ± 23*	282 ± 16*
750	367 ± 63*	400 ± 72*	406 ± 14*	431 ± 99*
875	340 ± 22*	379 ± 43*	392 ± 30*	397 ± 9*
1000	381 ± 5*	383 ± 80*	409 ± 36*	471 ± 45*
1100	355 ± 77*	433 ± 13*	482 ± 73*	534 ± 67*
6000	2703 ± 98*	3101 ± 814*	3019 ± 116**	3178 ± 436*

Note: * Concentration of 8:2 FTOH in nM and errors are reported as ± standard deviation. **One value was < LOD and was excluded from calculations for better regression (R^2) analysis.

Table S8. Levels of 8:2 FTOH versus time with the incubation of various 8:2 monoPAP concentrations in human fecal suspension (aerobic).

Concentration of 8:2 monoPAP incubated (nM)	45 min	50 min	55 min	60 min
500	319 ± 65*	324 ± 18*	326 ± 53*	326 ± 42*
750	357 ± 88*	378 ± 6*	387 ± 105*	404 ± 89*
875	573 ± 255*	620 ± 150*	641 ± 47*	629 ± 5*
1000	586 ± 83*	615 ± 360*,**	659 ± 213*	649 ± 105*
1100	545 ± 50*	508 ± 67*	580 ± 59*	642 ± 120*
6000	2741 ± 340*	n/a***	2884 ± 612*	3140 ± 491*

Note: * Concentration of 8:2 FTOH in nM and errors are reported as ± standard deviation. **One value was < LOD and was excluded from calculations for better regression (R^2) analysis. ***One value was <LOD and calculation based off n=2 greatly skewed the regression (R^2) analysis, and thus time point was excluded.

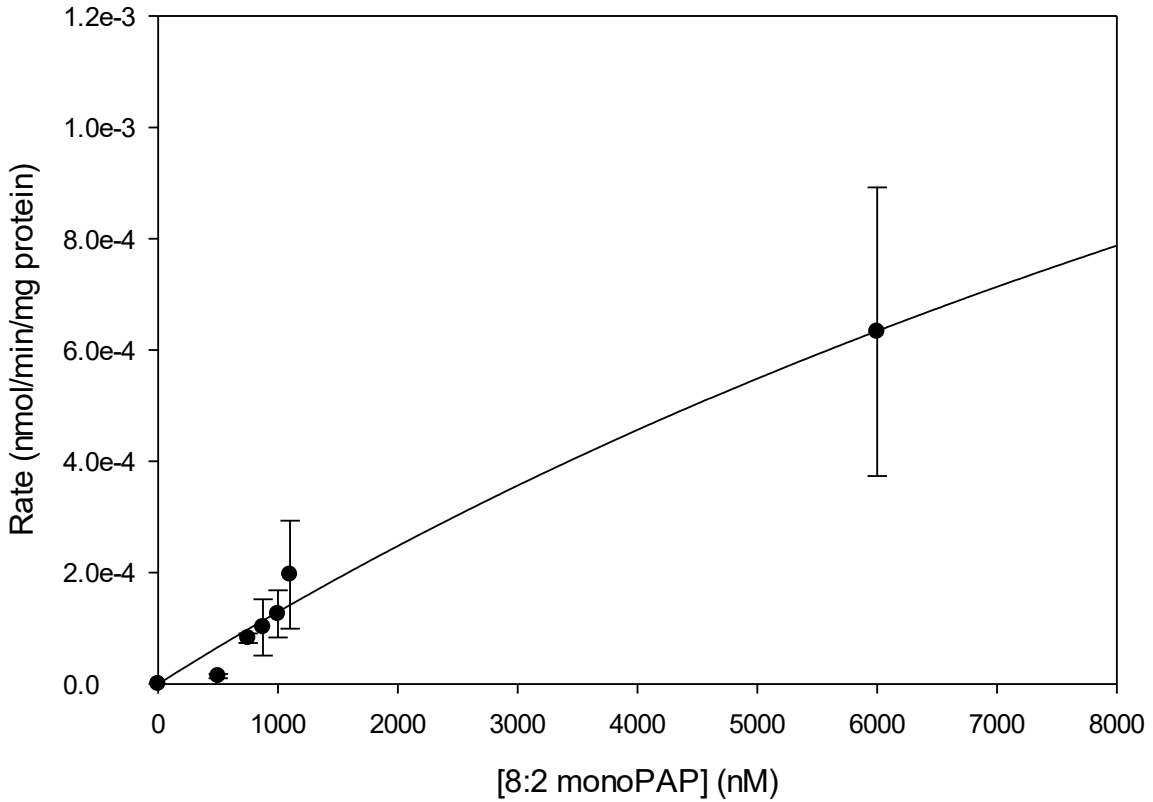

Figure S1. Michaelis Menten kinetics plots of 8:2 monoPAP (nM) versus biotransformation rate (nmol/min•mg) of protein in human feces (aerobic). V_{max} and K_M values were calculated from Systat Software SigmaPlot Version 14. All concentration points were performed in triplicates and error bars are reported as ± standard error.